Preprints.org

Bifurcation and Optimal Control Analysis of an HIV/AIDS Model with Saturated Incidence Rate

Marsudi Marsudi [*] , Trisilowati Trisilowati , Raqqasyi Rahmatullah Musafir

Article

Bifurcation and Optimal Control Analysis of an HIV/AIDS Model with Saturated Incidence Rate

Marsudi Marsudi [1,*], Trisilowati Trisilowati [1] and Raqqasyi R. Musafir [1]

[1] Department of Mathematics, Faculty of Mathematics and Natural Sciences, University of Brawijaya, Malang 65145, Indonesia

* Correspondence: marsudi61@ub.ac.id

Abstract: HIV/AIDS is a chronic disease that weakens the immune system if untreated. This study develops and analyzes an optimal control model of HIV/AIDS transmission with a saturated incidence rate to assess the effectiveness of time-dependent interventions. The model is described by seven nonlinear differential equations. We first establish that the model solutions are nonnegative and bounded. The existence and stability of equilibrium points are explored, and the effective reproduction number is derived using the next-generation matrix method. The Routh–Hurwitz criterion is applied to determine the local stability of the disease-free equilibrium, while center manifold theory is used to demonstrate the occurrence of a forward bifurcation and to analyze the local stability of the endemic equilibrium. Global stability is proven using the Castillo–Chavez method for the disease-free equilibrium and a Lyapunov function for the endemic equilibrium. Sensitivity analysis highlights the impact of parameter variations on disease dynamics, identifying the effective contact rate as the most influential parameter. The model is extended into an optimal control framework by introducing educational campaigns, screening, and antiretroviral treatment as control measures. The existence of optimal control is shown, and the Pontryagin Maximum Principle is used to derive optimal control. Numerical simulations support the theoretical findings, showing that combining multiple controls significantly reduces infection levels. A cost-effectiveness analysis identifies the combination of educational campaigns and antiretroviral treatment (Strategy C) as the most efficient intervention. Overall, the results yield important implications for formulating effective and economically sustainable HIV/AIDS intervention policies.

Keywords: HIV/AIDS model; saturated incidence; forward bifurcation; optimal control; cost-effectiveness

MSC: 34D23; 92D23; 49J15; 37N35

1. Introduction

The Human Immunodeficiency Virus (HIV) is a virus that attacks the body's immune system by targeting white blood cells, increasing susceptibility to infections such as tuberculosis and certain cancers, and continues to pose a serious global public health challenge, particularly when transmitted through unprotected sexual intercourse. Acquired Immunodeficiency Syndrome (AIDS) represents the most advanced stage of HIV infection, typically developing after years without treatment [1]. Prevention strategies are essential and include consistent and correct condom use, comprehensive sexual health education, and public education campaigns. Early diagnosis and the timely initiation of antiretroviral therapy (treatment) are crucial to controlling the infection and preventing progression to severe immunodeficiency, opportunistic infections, increased mortality, and reduced quality of life. Globally, an estimated 39.9 million people were living with HIV in 2023, with 1.3 million new cases. Sub-Saharan Africa remains the most affected region, accounting for over two-thirds of the global HIV burden. The global prevalence among adults aged 15-49 is about 0.6%, with women and girls representing 53% of all HIV cases [2]. Despite significant progress in expanding

access to antiretroviral therapy (ART), which now reaches 30.7 million people, the HIV epidemic continues to be a major public health issue. Timely screening and widespread ART availability are crucial to reducing transmission and improving health outcomes. The global spread of the HIV/AIDS epidemic has established it as a significant worldwide issue and an increasingly urgent public health challenge. The study of HIV/AIDS transmission dynamics has great attention from both mathematicians and biologists due to the multidimensional crisis, particularly in the health sector. To effectively accelerate HIV/AIDS prevention efforts, it is essential to integrate both behavioral and biomedical control strategies [3].

Due to its ability to provide both short-term and long-term forecasts of HIV and AIDS prevalence, the mathematical modelling approach has become an essential tool in analyzing the transmission and control of HIV/AIDS. There are many models in the literature that describe the dynamics of HIV/AIDS spread using a system of nonlinear differential equations. The model in [4–7], for example, incorporates behavior control through public education campaigns. These studies concluded that such campaigns, based on the ABC (Abstinence, Be faithful, use Condoms) strategy, can effectively reduce HIV/AIDS transmission. Antiretroviral treatment plays a crucial role in mitigating the spread of diseases such as HIV/AIDS. The model in [7] integrates behavioral intervention through education campaigns with biomedical treatment during the pre-AIDS stage. It introduces compartments for individuals practicing abstinence or faithfulness, condom users, and those under treatment. Thus, a compartmental HIV/AIDS model with seven population groups was developed to assess the impact of education campaigns and pre-AIDS treatment. The study used nonlinear differential equations to analyze stability and derive the effective reproduction number. The study concludes that treatment is the most effective among the three strategies. Furthermore, studies [8–10] indicate that well-designed public health education campaigns significantly influence HIV/AIDS transmission dynamics by highlighting their essential role in prevention efforts.

In mathematical epidemiology, disease incidence plays an important role in the study of epidemiological mathematical models. The incidence rate of disease is the rate at which new cases of infection appear in the population due to significant contact between susceptible individuals and infected individuals. Several types of incidence rates have been introduced in classical epidemiological modeling. The incidence rate of the form βSI is called the bilinear incidence rate. In contrast, the incidence of the form $\frac{\beta SI}{N}$, where β is the contact rate between susceptible and infected individuals, S is the number of susceptible individuals, I is the number of infectious individuals, and N is the total population, is known as the standard incidence rate [11]. Both types have been widely used in literature [7–10]. However, there are various reasons to modify these traditional incidence formulations. For instance, if the assumption of homogeneous mixing within the population does not hold, a nonlinear transmission function may be introduced to better reflect heterogeneous mixing and realistic population structures. A more accurate alternative is the saturated incidence rate, expressed as $\frac{\beta SI}{1+cI}$, which incorporates the inhibitory effect (c) associated with high levels of infective individuals. To capture the inhibitory effects arising from behavioral changes or the density of infected individuals, neither the mass action incidence nor the standard incidence function is sufficient. The saturated incidence form lies between the bilinear and standard incidence rates in terms of behavioral realism. Several mathematical models have been formulated using saturated functions to represent disease incidence or control measures such as treatment [12–16] and references therein.

Optimal control theory is a powerful tool for designing intervention strategies to minimize infection rates while considering implementation costs in epidemiological models [17,18]. This approach has been widely applied to HIV/AIDS dynamics. For example, Yusuf and Benyah [19] incorporated behavior change and antiretroviral therapy (ART), showing that early ART combined with behavioral interventions reduces HIV incidence and prevalence. Joshi et al. [4] emphasized the impact of information campaigns and awareness-based stratification in reducing HIV transmission. According to Safiel et al. [8], screening individuals unaware of their HIV status and treating identified cases are both effective in reducing the transmission of HIV/AIDS within a population. Building upon

this framework, Okosun et al. [9] extended this by including condom use, screening, and treatment in a time-dependent control model. Through the application of optimal control theory and cost-effectiveness analysis, the research highlighted the significant impact of awareness among infectives on disease transmission and associated costs. The findings concluded that the most cost-effective intervention involves the combined implementation of all control strategies. A related study [7] also examined the impact of information campaigns and treatment using optimal control and numerical simulations, confirming treatment as the most cost-effective strategy among those evaluated. The authors suggested incorporating the progression rate from asymptomatic infection to pre-AIDS as a control variable, given its high sensitivity index. Extending this to a co-infection setting, a model in [20,21] incorporated a protected class for HIV/AIDS and pneumonia, and a model in [22] incorporated a protected class and three time-dependent control measures for HIV and Hepatitis B Virus (HBV). The results show that integrating protective classes improves intervention outcomes and resource allocation. Collectively, these studies highlight the value of optimal control and cost-effectiveness analysis in guiding public health strategies to manage the transmission of diseases other than HIV/AIDS [23–29].

Motivated by the above studies, this study refers to the HIV/AIDS model presented in [7] by adding a screening intervention for the unaware infected individuals and assuming a saturation incidence rate. A deterministic compartmental model is proposed to capture the dynamics of HIV/AIDS transmission, followed by a comprehensive qualitative and quantitative analysis. Specifically, the study establishes the existence and stability of the disease-free and endemic equilibria and investigates the occurrence of bifurcations and their epidemiological implications. The model is further formulated as an optimal control problem by introducing time-dependent control variables representing educational campaigns, screening of unaware infectives, and treatment of aware infectives. The pairwise effectiveness of these controls is analyzed, and the most cost-effective strategy is identified using the Incremental Cost-Effectiveness Ratio (ICER) metrics. The novelty of this study lies in the comprehensive integration of three interventions (educational campaigns, screening, and treatment) into a unified modelling framework with saturated incidence. Additionally, the study evaluates the role of preventive interventions, including antiretroviral therapy, public health campaigns, and condom use, with particular emphasis on education for susceptible individuals, screening for the unaware infected, and treatment for the aware infected. By combining rigorous mathematical analysis with optimal control and cost-effectiveness evaluation, the study provides valuable insights for designing efficient and sustainable interventions for HIV/AIDS control.

This paper is organized as follows: Section 2 describes the formulation of a deterministic model for HIV/AIDS with a saturated incidence rate. In Section 3, we conduct a detailed analysis of the model, including its basic properties, the characterization of equilibrium points, and the derivation of the effective reproduction number. The section further investigates the local and global equilibria, bifurcation phenomena, and sensitivity analysis. In Section 4, the model is extended to an optimal control framework, and Pontryagin's Maximum Principle is employed to characterize the optimal control strategies. Section 5 presents numerical simulations based on selected parameter values to illustrate the analytical results of the model and includes a cost-effectiveness analysis of the proposed control strategies. Finally, Section 6 concludes the study with a summary of the key findings and potential directions for future research.

2. Formulation of the Model

In this section, we formulate a mathematical model for the transmission dynamics of HIV/AIDS in a population under the influence of three control strategies with a saturated incidence rate. The total human population, N is divided into seven compartments based on the epidemiological status of individuals, namely: S is the number of susceptible individuals, E_1 is the number of educated susceptible individuals who practice abstinence or be faithful (AB behavior), E_2 is the number of educated susceptible individuals who use condoms (C behavior), I_u is the number of unaware

infective individuals, I_a is the number of aware (screened) infective individuals, T is the number of individuals receiving antiretroviral (ARV) treatment, and A is the number of individuals at the critical stage of infection caused by HIV (full-blown AIDS). We consider a sexually active population, and the total population at time t is given by

$$N(t) = S(t) + E_1(t) + E_2(t) + I_u(t) + I_a(t) + T(t) + A(t).$$

Educational campaigns result in the division of the susceptible individuals S into three subclasses, with a proportion transitioning to E_1 and E_2 at the rate α_1 and α_2 is $\xi\alpha_1$ and $\xi\alpha_2$, where ξ is rate of educational campaigns. Susceptible individuals are uninfected but at risk of acquiring HIV through contact with three actively infectious classes, I_u, I_a, and T. The treated class consists of individuals receiving antiretroviral treatment for the screened infective class. The model assumes that the transmission follows a saturated incidence rate. The number of susceptible individuals S is assumed to increase at a new individuals enter the sexually active population at a constant recruitment rate Λ. Susceptible individuals are reduced by the force of infection

$$\lambda(I_u, I_a, T) = \frac{\beta(I_u + \eta_1 I_a + \eta_2 T)}{1 + \omega(I_u + I_a + T)},$$

where β is the effective contact rate, and $\eta_1, \eta_1 \in (0,1)$ is the modification parameter relative infectivity of individuals in I_u and I_a, respectively. The parameter that represents the psychological or inhibitory effect is denoted by ω. Moreover, susceptible individuals can become educated through education campaigns and move to the compartments E_1 and E_2 at a constant rate α_1 and α_2, respectively. It is further reduced by a natural death at a rate μ. Therefore, the rate of change of the susceptible individuals with time is given by

$$\frac{dS}{dt} = \Lambda - \lambda(I_u, I_a, T)S - (\xi\alpha_1 + \xi\alpha_2 + \mu)S. \tag{1}$$

The population of educated susceptible individuals who practice AB behavior increases as susceptible receive educational campaigns at a rate α_1, and decrease due to the force of infection at the rate $(1 - \psi_1)\lambda(I_u, I_a, T)$, where ψ_1 represents the effectiveness of these campaigns in promoting AB behavior. Additionally, the population is further reduced by natural death at a rate μ. Therefore, the rate of change of susceptible individuals practicing AB behavior due to educational campaigns is given by

$$\frac{dE_1}{dt} = \xi\alpha_1 S - (1 - \psi_1)\lambda(I_u, I_a, T)E_1 - \mu E_1. \tag{2}$$

The population of educated susceptible individuals who practice C behavior increases as susceptible receive educational campaigns at a rate α_2. It decreases due to the force of infection at the rate $(1 - \psi_2)\lambda(I_u, I_a, T)$, where ψ_2 denotes the effectiveness of the campaigns in promoting C behavior. This population also declines due to natural death at a rate μ. Therefore, the rate of change of susceptible individuals practicing C behavior because of educational campaigns is given by

$$\frac{dE_2}{dt} = \xi\alpha_2 S - (1 - \psi_2)\lambda(I_u, I_a, T)E_2 - \mu E_2. \tag{3}$$

The population of unaware infected individuals is generated by the force of infections $\lambda(I_u, I_a, T)$, $(1 - \psi_1)\lambda(I_u, I_a, T)$, and $(1 - \psi_2)\lambda(I_u, I_a, T)$. It decreases due to screening interventions among unaware infected individuals at a rate θ, and is further reduced by progression to full-blown AIDS at a rate σ_1, as well as by natural death at a rate μ. Thus, the rate of change of the unaware infected individuals is given by

$$\frac{dI_u}{dt} = \lambda(I_u, I_a, T)S + (1 - \psi_1)\lambda(I_u, I_a, T)E_1 + (1 - \psi_2)\lambda(I_u, I_a, T)E_2 - (\theta + \sigma_1 + \mu)I_u. \tag{4}$$

The population of aware infected individuals increases through screening of unaware infectives at a rate θ. This population decreases due to the intervention of antiretroviral treatment at a rate τ, and is further reduced by progression to full-blown AIDS at a rate σ_2, and natural death at a rate μ. Therefore, the rate of change of the aware individuals over time is given by

$$\frac{dI_a}{dt} = \theta I_u - (\tau + \sigma_2 + \mu) I_a \tag{5}$$

The population of treated infective individuals increases due to the intervention of antiretroviral treatment to aware infectives at a rate τ. This population decreases due to progression to full-blown AIDS at a rate σ_3 and natural death at a rate μ. Therefore, the rate of change of the treated infective individuals over time is given by

$$\frac{dT}{dt} = \tau I_a - (\sigma_3 + \mu) T. \tag{6}$$

The population of AIDS individuals increases due to the progression of unaware infectives, aware infectives, and treated individuals to the AIDS class, at rates $\sigma_1, \sigma_2,$ and σ_3 respectively. This population decreases due to natural death at a rate μ and further decreased by AIDS-induced death at a rate δ. Therefore, the rate of change of the full-blown AIDS individuals over time is given by

$$\frac{dA}{dt} = \sigma_1 I_u + \sigma_2 I_a + \sigma_3 T - (\delta + \mu) A. \tag{7}$$

A Compartment diagram of the HIV/AIDS model incorporating education campaigns, screening, and antiretroviral treatment interventions with saturated incidence rate is presented in Figure 1. Table 1 provides detailed descriptions of each model parameter.

Based on the compartmental diagram, the model describing the dynamics of HIV/AIDS transmission with a saturated incidence rate is represented by a seven-dimensional nonlinear system of ordinary differential equations, as shown in Equation (8).
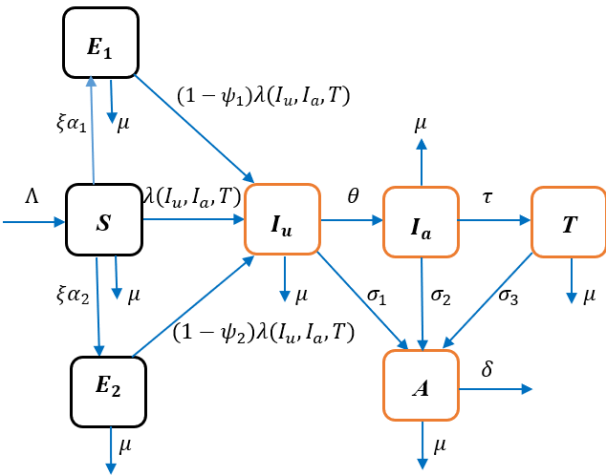

Figure 1. Compartment diagram for the HIV/AIDS model with saturated incidence rate.

Table 1. Description and the parameter values of the model (8).

Parameter	Description	Value	Source
Λ	Rate of recruitment	2000	[6]
μ	Natural death rate	0.0196	[6]
θ	The rate of screening of unaware infective	0.6	[6]
ψ_1	The efficiency of education campaigns in E_1	0.75	Assumed
ψ_2	The efficiency of education campaigns in E_2	0.6	Assumed

ξ	The rate of educating adults into E1	0.4	[6]
α_1	The rate of educating adults into E_1	0.091	Assumed
α_2	The rate of educating adults into E_2	0.067	Assumed
τ	The rate of treatment of aware infectious	0.6	[9]
σ_1	Progression rate from unaware infectious to AIDS	0.1	[8]
σ_2	Progression rate from aware infectious to AIDS	0.01	[8]
σ_3	Progression rate from treated infection to AIDS	0.001	[8]
η_1	The modification parameter relative infectivity of individuals in I_a	0.023	Assumed
η_2	The modification parameter relative infectivity of individuals in T	0.0016	Assumed
δ	The rate of treatment of screened infectious	0.33	[6]
ω	The psychological or inhibitory effect	4	[10]

$$\frac{dS}{dt} = \Lambda - \lambda(I_u, I_a, T)S - (\xi\alpha_1 + \xi\alpha_2 + \mu)S,$$

$$\frac{dE_1}{dt} = \xi\alpha_1 S - (1-\psi_1)\lambda(I_u, I_a, T)E_1 - \mu E_1,$$

$$\frac{dE_2}{dt} = \xi\alpha_2 S - (1-\psi_2)\lambda(I_u, I_a, T)E_2 - \mu E_2,$$

$$\frac{dI_u}{dt} = \lambda(I_u, I_a, T)S + (1-\psi_1)\lambda(I_u, I_a, T)E_1 + (1-\psi_2)\lambda(I_u, I_a, T)E_2 - (\theta + \sigma_1 + \mu)I_u, \qquad (8)$$

$$\frac{dI_a}{dt} = \theta I_u - (\tau + \sigma_2 + \mu)I_a,$$

$$\frac{dT}{dt} = \tau I_a - (\sigma_3 + \mu)T,$$

$$\frac{dA}{dt} = \sigma_1 I_u + \sigma_2 I_a + \sigma_3 T - (\delta + \mu)A.$$

with nonnegative initial conditions,

$$S(0) = S^0, E_1(0) = E_1^0, E_2(0) = E_2^0, I_u(0) = I_u^0,$$
$$I_a(0) = I_a^0, T(0) = T^0, A(0) = A^0. \qquad (9)$$

3. Analysis of the Model

3.1. Positivity and Boundedness of Solutions

Lemma 1. *If* $S(0), E_1(0), E_2(0), I_u(0), I_a(0), T(0), A(0)$ *are nonnegative, then the solutions of the model (8) are nonnegative for all* $t \geq 0$.

Proof. To prove this, we employ a proof by contradiction to demonstrate that each state variable remains non-negative for all $t \geq 0$. Let us denote

$$m(t) = \min\{S(t), E_1(t), E_2(t), I_u(t), I_a(t), T(t), A(t)\}.$$

Given that all initial conditions are nonnegative, it follows that $m(0) \geq 0$. Without loss of generality, assume $m(t) = S(t)$. We will use proof by contradiction to show that $S(t) \geq 0$ for all $t \geq 0$. Suppose on the contrary, that this is not the case. Then, there exists a first time t_1 such that hold

$$S(t_1 - \varepsilon) \geq 0, \ S(t_1) = 0, \ \text{and} \ S(t_1 + \varepsilon) < 0, \qquad (10)$$

for some positive constant ε. From the first equation of model (8) and evaluating at t_1, we have

$$\frac{dS(t_1)}{dt} = \Lambda - \lambda(I_u(t_1), I_a(t_1), T(t_1))S(t_1) - (\xi\alpha_1 + \xi\alpha_2 + \mu)S(t_1).$$

Since $\Lambda > 0$ and $S(t_1) = 0$, this simplifies to

$$\frac{dS(t_1)}{dt} = \Lambda > 0$$

By the Monotonicity Theorem, it follows that $S(t_1 + \varepsilon) \geq 0$ for all $\varepsilon > 0$, which contradicts the assumption in Equation (10) that $S(t_1 + \varepsilon) < 0$. Therefore, the contradiction implies that $S(t) \geq 0$ for all t $\geq$ 0Using a similar argument, it can be shown that $E_1(t) \geq 0$, $E_2(t) \geq 0$, $I_u(t) \geq 0$, $I_a(t) \geq 0$, $T(t) \geq 0$, and $A(t) \geq 0$ for all t $\geq$ 0. This completes the proof. $\square$

Lemma 2. Solution of the model (8) with nonnegative initial values are bounded.

Proof. Let $(S, E_1, E_2, I_u, I_a, T, A) \in R_+^7$ is an arbitrary non-negative solution of the model (8) with initial conditions given in Equation (9). The total population $N(t) = S(t) + E_1(t) + E_2(t) + I_u(t) + I_a(t) + T(t) + I(t)$. Now adding all the differential equations given in Equation (1) we have got the derivative of the total population $N(t)$ to time t, we have

$$\frac{dN(t)}{dt} = \Lambda - \mu N(t) - \delta A(t).$$

Next, disregarding the infections $A(t)$, we have determined that

$$\frac{dN(t)}{dt} \leq \Lambda - \mu N(t). \tag{11}$$

Thus, for the initial condition $0 \leq N \leq \frac{\Lambda}{\mu}$, and by applying the Standard Comparison Theorem [30], we get

$$0 \leq N(t) \leq \frac{\Lambda}{\mu}. \tag{12}$$

Therefore, the solutions $S(t), E_1(t), E_2(t), I_u(t), I_a(t), T(t)$, and $A(t)$ of the model (8) are bounded above by Λ/μ. This completes the proof. $\square$

Hence, the biologically feasible region of the HIV/AIDS model (8) is given the following positively invariant region:

$$\Omega = \left\{ (S, E_1, E_2, I_u, I_a, T, A) \in \mathbb{R}_+^7 \mid 0 \leq S + E_1 + E_2 + I_u + I_a + T + A \leq \frac{\Lambda}{\mu} \right\}.$$

3.2. Existence of Equilibrium Points

To compute the equilibrium solutions of the model (8), we set the right-hand sides of the equations for model (8) to zero.

3.2.1. Disease-Free Equilibrium (DFE) and Effective Reproduction Number

The disease-free equilibrium (DFE) of the HIV/AIDS model (8) is given by

$$\mathcal{E}_0 = \left(S^0, E_1^0, E_2^0, I_u^0, I_a^0, T^0, A^0 \right)$$
$$= \left(\frac{\Lambda}{\xi\alpha_1 + \xi\alpha_2 + \mu}, \frac{\xi\alpha_1\Lambda}{\mu(\xi\alpha_1 + \xi\alpha_2 + \mu(\xi\alpha_1 + \xi\alpha_2 + \mu)}, \frac{\xi\alpha_2\Lambda}{\mu(\xi\alpha_1 + \xi\alpha_2 + \mu)}, 0, 0, 0, 0 \right) \tag{13}$$

To determine the effective reproduction number for model (8), we employ the next-generation matrix method as presented in [31]. Following the approach described in [31,32], we construct the matrix $\mathcal{F}$ and $\mathcal{V}$, which represent the matrix of new infections and transition matrix between the

compartments of the system, respectively. Considering the infected compartments $x = (I_u, I_a, T, A)^T$, the right-hand side of model (8) can be rewritten by

$$\frac{dx}{dt} = \mathcal{F}(x) - \mathcal{V}(x) \tag{14}$$

where

$$\mathcal{F} = \begin{bmatrix} \lambda(I_u, I_a, T)S + c_1\lambda(I_u, I_a, T)E_1 + c_2(I_u, I_a, T)\lambda E_2 \\ 0 \\ 0 \\ 0 \end{bmatrix}, \quad \mathcal{V} = \begin{bmatrix} LI_u \\ -\theta I_u + MI_a \\ -\tau I_a + WT \\ -\sigma_1 I_u - \sigma_2 I_a - \sigma_3 T + PA \end{bmatrix}.$$

The matrix F is the Jacobian matrix of $\mathcal{F}$ evaluated at the disease-free equilibrium $\mathcal{E}_0$, and the matrix V is the Jacobian matrix of $\mathcal{V}$ evaluated at the disease-free equilibrium $\mathcal{E}_0$, we have

$$F = \begin{bmatrix} \frac{\beta Q \Lambda}{\mu K} & \frac{\beta \eta_1 Q \Lambda}{\mu K} & \frac{\beta \eta_2 Q \Lambda}{\mu K} & 0 \\ 0 & 0 & 0 & 0 \\ 0 & 0 & 0 & 0 \\ 0 & 0 & 0 & 0 \end{bmatrix} \text{ and } V = \begin{bmatrix} L & 0 & 0 & 0 \\ -\theta & M & 0 & 0 \\ 0 & -\tau & W & 0 \\ -\sigma_1 & -\sigma_2 & -\sigma_3 & P \end{bmatrix}. \tag{15}$$

The next-generation matrix (FV^{-1}) is

$$FV^{-1} = \begin{bmatrix} \frac{\beta \Lambda Q}{\mu KL} + \frac{\beta \Lambda \eta_1 \theta Q}{\mu KLM} + \frac{\beta \Lambda \eta_2 \theta \tau Q}{\mu KLMW} & \frac{\beta \Lambda \eta_1 Q}{\mu KM} + \frac{\beta \Lambda \eta_2 \tau Q}{\mu KMW} & \frac{\beta \Lambda \eta_1 Q}{\mu KW} & 0 \\ 0 & 0 & 0 & 0 \\ 0 & 0 & 0 & 0 \\ 0 & 0 & 0 & 0 \end{bmatrix}$$

where

$$K = \xi\alpha_1 + \xi\alpha_2 + \mu, L = \theta + \sigma_1 + \mu, M = \tau + \sigma_2 + \mu, W = \sigma_3 + \mu, P = \delta + \mu, c_1 = 1 - \psi_1, c_2 = 1 - \psi_2,$$
$$Q = c_1\xi\alpha_1 + c_2\xi\alpha_2 + \mu.$$

Hence, the effective reproduction number of model (8) is defined as the maximum of the absolute values of the eigenvalues of the next-generation matrix, FV^{-1} given by

$$\mathcal{R}_e = \frac{\beta \Lambda Q}{\mu KL} + \frac{\beta \Lambda \eta_1 \theta Q}{\mu KLM} + \frac{\beta \Lambda \eta_2 \theta \tau Q}{\mu KLMW} = \mathcal{R}_{I_u} + \mathcal{R}_{I_a} + \mathcal{R}_T, \tag{16}$$

where $\mathcal{R}_{I_u} = \frac{\beta \Lambda Q}{\mu KL}$, $\mathcal{R}_{I_a} = \frac{\beta \Lambda Q \eta_1 \theta}{\mu KLM}$, and $\mathcal{R}_T = \frac{\beta \Lambda Q \eta_2 \theta \tau}{\mu KLMW}$. Here, $\mathcal{R}_{I_u}$ is the contribution to the reproduction number with intervention by unaware infective individuals I_u, $\mathcal{R}_{I_a}$ is the contribution to the reproduction number with intervention by aware (screened) infective individuals I_a, and $\mathcal{R}_T$ is the contribution to the reproduction number with treated individuals T.

When education campaigns, screening, and treatment are implemented to control and eradicate the disease, the effective reproduction number represents the average number of new infections generated by a single HIV-infected individual in a susceptible population, under the influence of these control strategies.

3.2.2. Existence of Endemic Equilibrium

In this subsection, we will find conditions for the existence of an endemic equilibrium (EE) for the model (8). Let's determine the effective reproduction number. The equilibrium of model (8) and its stability denote an arbitrary endemic equilibrium of model (8). Solving the equilibrium conditions of the model (8) at a steady state gives

$$S^* = \frac{\Lambda}{\lambda^* + K}, E_1^* = \frac{\xi\alpha_1\Lambda}{(c_1\lambda^* + \mu)(\lambda^* + K)}, E_2^* = \frac{\xi\alpha_2\Lambda}{(c_2\lambda^* + \mu)(\lambda^* + K)},$$

$$I_u^* = \frac{\lambda^*\Lambda}{L(\lambda^* + K)} + \frac{c_1\lambda^*\xi\alpha_1\Lambda}{L(c_1\lambda^* + \mu)(\lambda^* + K)} + \frac{c_2\lambda^*\xi\alpha_2\Lambda}{L(c_2\lambda^* + \mu)(\lambda^* + K)}, \tag{17}$$

$$I_a^* = y_1 I_u^*, T^* = y_2 I_u^*, A^* = y_3 I_u^*,$$

where $y_1 = \frac{\theta}{M}$, $y_2 = \frac{\theta\tau}{MW}$, $y_3 = \frac{\sigma_1 + \sigma_2 y_1 + \sigma_3 y_2}{P}$, and

$$\lambda^* = \frac{\beta(I_u^* + \eta_2 I_a^* + \eta_3 T^*)}{1 + \omega(I_u^* + I_a^* + T^*)} \tag{18}$$

Substituting the value of I_u^*, I_a^*, T^* in (17) into (18), we obtain

$$\lambda^*(a_3\lambda^{*3} + a_2\lambda^{*2} + a_1\lambda^* + a_0) = 0, \tag{19}$$

where

$$a_3 = c_1 c_2[\Lambda\omega(1 + y_1 + y_2) + L],$$

$$a_2 = [\Lambda\omega(c_1 c_2 \xi(\alpha_1 + \alpha_2) + (c_1 + c_2)\mu)](1 + y_1 + y_2) - \Lambda c_1 c_2\beta(1 + \eta_1 y_1 + \eta_2 y_2)$$

$$+ L[\mu(c_1 + c_2) + Qc_1 c_2],$$

$$a_1 = \Lambda\omega\mu Q(1 + y_1 + y_2) + L\mu[K(c_1 + c_2) + \mu] - \Lambda\beta[c_1 c_2\xi(\alpha_1 + \alpha_2) + (c_1 + c_2)\mu](1 + \eta_1 y_1 + \eta_2 y_2),$$

$$a_0 = LK\mu^2(1 - \mathcal{R}_e).$$

From Equation (19), one solution is $\lambda^* = 0$ corresponds to the disease-free equilibrium. Another solution is given by the roots of a cubic polynomial (20),

$$a_3\lambda^{*3} + a_2\lambda^{*2} + a_1\lambda^* + a_0 = 0, \tag{20}$$

which is related to situations where the HIV disease persists. For the endemic equilibrium to exist, λ^* is a positive real root of the cubic polynomial (20). It is clear that $a_3 > 0$ (since all model parameters are nonnegative) and $a_0 < 0$ when $\mathcal{R}_e > 1$. Thus, the number of possible positive real roots of the cubic polynomial (20) depends on the signs of a_1 and a_2. By applying Descarte's Rule of Signs to the cubic polynomial in Equation (20), the number of positive real roots can be determined. In addition, according to [7], using Cardan's formula, the polynomial (13) has one positive real root and a pair of complex conjugate roots if the discriminant $\Delta = r^2 + q^3 > 0$, given by

$$\lambda_1^* = u + v - \frac{a_2}{3a_3}, \lambda_2^* = -\frac{u+v}{2} - \frac{a_2}{3a_3} + \frac{i\sqrt{3}(u-v)}{2}, \lambda_3^* = -\frac{u+v}{2} - \frac{a_2}{3a_3} - \frac{i\sqrt{3}(u-v)}{2}, \tag{21}$$

where $u = \sqrt[3]{r + \sqrt{r^2 + q^3}}$, $v = \sqrt[3]{r - \sqrt{r^2 + q^3}}$, and $q = \frac{3a_3 a_1 - a_2^2}{9a_3^2}$, $r = \frac{9a_3 a_2 a_1 - 27a_3^2 a_0 - 2a_2^2}{54a_3^2}$.

Furthermore, if Equation (20) has a single positive real root, then the components of the endemic equilibrium $\mathcal{E}_1 = (S^*, E_1^*, E_2^*, I_u^*, I_a^*, T^*, A^*)$ can be obtained by substituting the value of $\lambda = \lambda_1^*$ into the expression for each state in Equation (20). This result is summarized in the following lemma.

Lemma 3. *The model (8) has a unique endemic equilibrium $\mathcal{E}_1$ whenever $\mathcal{R}_e > 1$ with $\lambda = \lambda_1^*$ are the positive real roots of Equation (20).*

3.3. Stability Analysis

3.3.1. Local Stability of Disease-Free Equilibrium

Theorem 1. *The disease-free equilibrium of the model (8),* $\mathcal{E}_0$ *, is locally asymptotically stable if* $\mathcal{R}_e < 1$, *and unstable if* $\mathcal{R}_e > 1$.

Proof. The Jacobian matrix of the model (8) at the disease-free equilibrium $\mathcal{E}_0$, denoted by $J(\mathcal{E}_0)$ is given as

$$J(\mathcal{E}_0) = \begin{pmatrix} -K & 0 & 0 & -\frac{\beta\Lambda}{K} & -\frac{\beta\Lambda\eta_1}{K} & -\frac{\beta\Lambda\eta_2}{K} & 0 \\ \xi\alpha_1 & -\mu & 0 & -\frac{\beta\Lambda c_1\xi\alpha_1}{\mu K} & -\frac{\beta\Lambda\eta_1 c_1\xi\alpha_1}{\mu K} & -\frac{\beta\Lambda\eta_2 c_1\xi\alpha_1}{\mu K} & 0 \\ \xi\alpha_2 & 0 & -\mu & -\frac{\beta\Lambda c_2\xi\alpha_2}{\mu K} & -\frac{\beta\Lambda\eta_1 c_2\xi\alpha_2}{\mu K} & -\frac{\beta\Lambda\eta_2 c_2\xi\alpha_2}{\mu K} & 0 \\ 0 & 0 & 0 & \frac{\beta\Lambda Q}{\mu K} - L & \frac{\beta\Lambda\eta_1 Q}{\mu K} & \frac{\beta\Lambda\eta_2 Q}{\mu K} & 0 \\ 0 & 0 & 0 & \theta & -M & 0 & 0 \\ 0 & 0 & 0 & 0 & \tau & -W & 0 \\ 0 & 0 & 0 & \sigma_1 & \sigma_2 & \sigma_3 & -P \end{pmatrix}. \tag{22}$$

There are seven eigenvalues of the matrix $J(\mathcal{E}_0)$; four of the eigenvalues are $\lambda_1 = \lambda_2 = -\mu, \lambda_3 = -K, \lambda_4 = -P$, and the remaining eigenvalues are the solutions of the following into the 3×3 matrix as shown below,

$$J_1 = \begin{pmatrix} \frac{\beta\Lambda Q}{\mu K} - L & \frac{\beta\Lambda\eta_1 Q}{\mu K} & \frac{\beta\Lambda\eta_2 Q}{\mu K} \\ \theta & -M & 0 \\ 0 & \tau & -W \end{pmatrix}. \tag{23}$$

The characteristic equational corresponding to J_1 is

$$\lambda^{*3} + h_1\lambda^{*2} + h_2\lambda^* + h_3 = 0, \tag{24}$$

where

$$h_1 = L(1 - \mathcal{R}_{I_u}) + M + W,$$

$$h_2 = LM(1 - \mathcal{R}_{I_a}) + W(L + M) - \mathcal{R}_{I_u}(M + W),$$

$$h_3 = LMW(1 - \mathcal{R}_e).$$

As $-\mu, -K, -P$ are negative, the Routh-Hurwitz Criteria depicted that, Equation (24) has three negative roots if $h_1 > 0, h_2 > 0, h_3 > 0$, and $h_1 h_2 > h_3$. Thus, this is possible only $\mathcal{R}_e < 1$. As a result, the disease-free equilibrium of the model (8), $\mathcal{E}_0$, is locally asymptotically stable in Ω if $\mathcal{R}_e < 1$. If $\mathcal{R}_e > 1$, the Jacobian matrix $J(\mathcal{E}_0)$ has at least one eigenvalue with a positive real part. Thus, the disease-free equilibrium $\mathcal{E}_0$ is locally asymptotically unstable. This completes the proof. $\square$

3.3.2. Global Stability of Disease-Free Equilibrium

To establish the global stability of the disease-free equilibrium $\mathcal{E}_0$, we apply the method used in [33]. To do this, let the model (8) be rewritten in the form

$$\frac{dX}{dt} = F(X,Y),$$

$$\frac{dZ}{dt} = G(X,Z), G(X,0) = 0,$$

(25)

where $X = (S, E_1, E_2) \in \mathbb{R}^3$ is the uninfected compartments, $Z = (I_u, I_a, T, A) \in \mathbb{R}^4$ is the infected compartments. Let $\mathcal{E}_0 = (X^0, 0, 0, 0, 0)$, where $X^0 = \left(S^0, E_1^0, E_2^0\right)$ denotes the disease-free equilibrium of model (8). To establish the global asymptotic stability of the disease-free equilibrium of model (8), the following conditions must be satisfied:

(H_1) For $\frac{dX}{dt} = F(X,0)$, X^0 is globally asymptotically stable.

(H_2) $G(X,Z) = BZ - \hat{G}(X,Z), G(X,Z) \geq 0$ for $(X, Z) \in \Omega$ and $B = D_Z G(X^0, 0)$ is a Metzler-matrix (the off-diagonal elements of B are nonnegative).

Theorem 2. *The disease-free equilibrium points of the model $\mathcal{E}_0$ is globally asymptotically stable for $\mathcal{R}_e < 1$.*

Proof. System (8) can be written as the system (25) form, and we get $X = (S, E_1, E_2) \in \mathbb{R}^3$, $Z = (I_u, I_a, T, A) \in \mathbb{R}^4$. Next, we have identified the following matrices:

$$F(X,Z) = \begin{pmatrix} \Lambda - \frac{\beta(I_u + \eta_1 I_a + \eta_2 T)}{1 + \omega(I_u + I_a + T)} S - KS \\ \xi\alpha_1 S - \frac{\beta(I_u + \eta_1 I_a + \eta_2 T)}{1 + \omega(I_u + I_a + T)} c_1 E_1 - \mu E_1 \\ \xi\alpha_2 S - \frac{\beta(I_u + \eta_1 I_a + \eta_2 T)}{1 + \omega(I_u + I_a + T)} c_2 E_2 - \mu E_2 \end{pmatrix}, G(X,Z) = \begin{pmatrix} \frac{\beta(I_u + \eta_1 I_a + \eta_2 T)}{1 + \omega(I_u + I_a + T)}(S + c_1 E_1 + c_2 E_2) - LI_u \\ \theta I_u - MI_a \\ \tau I_a - WT \\ \sigma_1 I_u + \sigma_2 I_a + \sigma_3 T - PA \end{pmatrix}.$$

From the first equation of system (25),

$$\frac{dX}{dt} = F(X,0) = \begin{pmatrix} \Lambda - KS \\ \xi\alpha_1 S - \mu E_1 \\ \xi\alpha_2 S - \mu E_2 \end{pmatrix}.$$

(26)

The Jacobian matrix of $F(X,0)$ is given by

$$J(F(X,0)) = \begin{pmatrix} -K & 0 & 0 \\ \xi\alpha_1 & -\mu & 0 \\ \xi\alpha_2 & 0 & -\mu \end{pmatrix}.$$

(27)

The eigen values of the matrix $J(F(X,0))$ in system (27) are $-K, -\mu$, and $-\mu$. Since the eigenvalues of the given matrix (27) are clearly negative, then the system (26) is globally asymptotically stable. At $F(X,0) = 0$, $X^0 = \left(S^0, E_1^0, E_2^0\right) = \left(\frac{\Lambda}{K}, \frac{\xi\alpha_1\Lambda}{\mu K}, \frac{\xi\alpha_2\Lambda}{\mu K}\right)$. As $t \to \infty$, $S \to S^0, E_1 \to E_1^0, E_2 \to E_2^0$. Thus, condition ($H_1$) is satisfied and X^0 is globally asymptotically stable. Additionally, we demonstrate that $G(X, Z)$ satisfies the second requirements stated in (H_2). It is clear that $G(X, 0) = 0$. We derive from the second equation in Equation (25),

$$B = D_X G(X^0, 0)$$

$$= \begin{pmatrix} \beta(S^0 + c_1 E_1^0 + c_2 E_2^0) - L & \beta\eta_1(S^0 + c_1 E_1^0 + c_2 E_2^0) & \beta\eta_2(S^0 + c_1 E_1^0 + c_2 E_2^0) & 0 \\ \theta & -M & 0 & 0 \\ 0 & \tau & -W & 0 \\ \sigma_1 & \sigma_2 & \sigma_3 & -P \end{pmatrix}. \text{(28)}$$

.

B is a Metzler-matrix because all off-diagonal entries of the matrix B are not negative and

$$\hat{G}(X,Z) = BZ - G(X,Z)$$

$$= \begin{pmatrix} \beta(I_u + \eta_1 I_a + \eta_2 T)[\frac{(S^0-S)+\omega(I_u+I_a+T)S^0}{1+\omega(I_u+I_a+T)} + c_1(\frac{(E_1^0-E_1)+\omega(I_u+I_a+T)E_1^0}{1+\omega(I_u+I_a+T)} + c_2(\frac{(E_2^0-E_2)+\omega(I_u+I_a+T)E_2^0}{1+\omega(I_u+I_a+T)})] \\ 0 \\ 0 \\ 0 \\ 0 \\ 0 \end{pmatrix}.$$

Clearly, $\hat{G}(X,Z) \geq 0$ is true, since $0 \leq S \leq S^0, 0 \leq E_1 \leq E_1^0, 0 \leq E_2 \leq E_2^0$. As a result, condition (H$_2$) is satisfied. Therefore, both conditions are satisfied, and the proof of Theorem 2 is completed. □

3.3.3. Global Stability of Endemic Equilibrium

To analyze the global dynamics of model (8) around the unique endemic equilibrium point $\mathcal{E}_1$, we present the following result.

Theorem 3. *If $\mathcal{R}_e > 1$, then the endemic equilibrium $\mathcal{E}_1$ of the model (8) is globally asymptotically stable in Ω.*

Proof of Theorem 3. Let $\mathcal{R}_e > 1$ such that the endemic equilibrium $\mathcal{E}_1$ exist. Furthermore, considering the following function $\mathcal{L}_2$, inspired by Muthu and Kumar [34] as follows:

$$\mathcal{L}_2 = (S + E_1 + E_2 + I_u + I_a + T + A) - (S^* + E_1^* + E_2^* + I_u^* + I_a^* + T^* + A^*)$$

$$- (S^* + E_1^* + E_2^* + I_u^* + I_a^* + T^* + A^*)\ln\left(\frac{S+E_1+E_2+I_u+I_a+T+A}{S^*+E_1^*+E_2^*+I_u^*+I_a^*+T^*+A^*}\right) \qquad (29)$$

$$= N - N^* - N^*\ln\left(\frac{N}{N^*}\right).$$

By direct calculating the derivative of $\mathcal{L}_2$ with respect to t along the solutions of the model (8), we have

$$\frac{d\mathcal{L}_2}{dt} = \left(1 - \frac{N^*}{N}\right)\frac{dN}{dt} = \left(1 - \frac{N^*}{N}\right)(\Lambda - \delta A - \mu N).$$

From the right-hand sides of (5) at steady state, we have $\Lambda = \delta A^* + \mu N^*$. Thus,

$$\frac{d\mathcal{L}_2}{dt} = \left(1 - \frac{N^*}{N}\right)(\delta A^* + \mu N^* - \delta A - \mu N) = \frac{N-N^*}{N}\left(-\mu(N-N^*) - \delta(A-A^*)\right)$$

$$= -\frac{\mu(N^*-N)^2}{N} - \frac{\delta(N^*-N)(A^*-A)}{N}. \qquad (30)$$

Clearly, $d\mathcal{L}_2/dt < 0$ because $S \leq S^*, E_1 \leq E_1^*, E_2 \leq E_2^*, I_u \leq I_u^*, I_a \leq I_a^*, T \leq T^*, A \leq A^*$, which implies $0 \leq N \leq N^*$. Additionally, $d\mathcal{L}_2/dt = 0$ if and only if $S = S^*, E_1 = E_1^*, E_2 = E_2^*$, $I_u = I_u^*, I_a = I_a^*, T = T^*, A = A^*$. Hence, $\mathcal{L}_2$ is a Lyapunov function on   Thus, $S_1 \to S^*$, $E_1 \to E_1^*, E_2 \to E_2^*, I_1 \to I_1^*, I_2 \to I_2^*, T \to T^*, A \to A^*$ as $t \to \infty$. Therefore, the largest compact invariant set in $\{(S, E_1, E_2, I_u, I_a, T, A) \in \Omega \mid \frac{d\mathcal{L}_2}{dt} = 0\}$ is the singleton set $\{\mathcal{E}_1\}$. By LaSalle's Invariance Principle [35], the unique endemic equilibrium of the model (8) is globally asymptotically stable in Ω. The proof of Theorem 3 is completed. □

The epidemiological implication of the above result is that the HIV/AIDS epidemic will persist in the community despite education campaigns, screening, and antiretroviral treatment programs if the threshold quantity ($\mathcal{R}_e$) exceeds unity.

3.4. Bifurcation Analysis

An important phenomenon in compartmental epidemiological modelling, particularly in HIV/AIDS transmission, is the occurrence of a bifurcation at the critical point where $\mathcal{R}_e = 1$. To investigate the existence of a bifurcation for the model (8), we employ the center manifold theory as described by Castillo-Chavez and song in [33].

Theorem 4. *The HIV/AIDS model (8) exhibits a forward bifurcation at* $\mathcal{R}_e = 1$ *whenever* $B_0 < 0$ *holds, with*

$$B_0 = \left(K\beta^*\xi\left(\alpha_1 c_1\psi_1 + \alpha_2 c_2\psi_2\right) + \beta^*\mu\xi\left(\alpha_1 + \alpha_2\right)\right)\left(W\eta_1\theta + \eta_2\tau\theta + MW\right)$$
$$+ K\mu\omega\left(W\theta\xi + MW + \tau\theta\right)\left(\alpha_1\psi_1 + \alpha_2\psi_2\right)$$
$$- \left(K\beta^*\xi\left(\alpha_1 c_1 + \alpha_2 c_2\right) + \beta^*\mu\xi\left(\alpha_1\psi_1 + \alpha_2\psi_2\right) + \beta^*\mu^2\right)\left(W\eta_1\theta + MW + \eta_2\tau\theta\right)$$
$$- K\mu^2\omega\left(MW + W\theta + \tau\theta\right) - K\theta\xi\mu\omega\left(MW + \tau + W\right)\left(\alpha_1 + \alpha_2\right).$$

Proof of Theorem 4. We simplify model (8) by choosing, $S = x_1, E_1 = x_2, E_2 = x_3, I_u = x_4,$ $I_a = x_5, T = x_6, A = x_7$. If we set, $X = \left(x_1, x_2, x_3, x_4, x_5, x_6, x_7\right)^T$, then our model (8) can be written in the form $\frac{dX}{dt} = f(X)$ with $f = (f_1, f_2, f_3, f_4, f_5, f_6, f_7)^T$. Thus, we have

$$f_1 = \Lambda - \left(\frac{\beta(x_4 + \eta_1 x_5 + \eta_2 x_6)}{1 + \omega(x_4 + x_5 + x_6)}\right)x_1 - Kx_1,$$
$$f_2 = \xi\alpha_1 x_1 - c_1\left(\frac{\beta(x_4 + \eta_1 x_5 + \eta_2 x_6)}{1 + \omega(x_4 + x_5 + x_6)}\right)x_2 - \mu x_2,$$
$$f_3 = \xi\alpha_2 x_1 - c_2\left(\frac{\beta(x_4 + \eta_1 x_5 + \eta_2 x_6)}{1 + \omega(x_4 + x_5 + x_6)}\right)x_3 - \mu x_3,$$
$$f_4 = \left(\frac{\beta(x_4 + \eta_1 x_5 + \eta_2 x_6)}{1 + \omega(x_4 + x_5 + x_6)}\right)x_1 + c_1\left(\frac{\beta(x_4 + \eta_1 x_5 + \eta_2 x_6)}{1 + \omega(x_4 + x_5 + x_6)}\right)x_2 + c_2\left(\frac{\beta(x_4 + \eta_1 x_5 + \eta_2 x_6)}{1 + \omega(x_4 + x_5 + x_6)}\right)x_3,$$
$$f_5 = \theta x_4 - Mx_5,$$
$$f_6 = \tau x_5 - Wx_6,$$
$$f_7 = \sigma_1 x_4 + \sigma_2 x_5 + \sigma_3 x_6 - Px_7.$$

The characteristic equation in Equation (20) produces an eigenvalue of zero if $h_3 = LMW(1 - \mathcal{R}_e)$. We simplify this equation and considering $\mathcal{R}_e$ stated in Equation (16), we get $\mathcal{R}_e = 1$. By selecting β as the bifurcation parameter at the point where $\mathcal{R}_e = 1$, we obtain the critical value of β as follows:

$$\beta = \beta^* = \frac{\mu KLMW}{\Lambda Q(MW + \eta_1\theta W + \eta_2\theta\tau)}, \tag{31}$$

The Jacobian matrix of the model (8), evaluated at the disease-free equilibrium $\mathcal{E}_0$ and $\beta = \beta^*$, is given by

$$J(\mathcal{E}_0, \beta^*) = \begin{pmatrix} -K & 0 & 0 & -\frac{\beta^*\Lambda}{K} & -\frac{\beta^*\Lambda\eta_1}{K} & -\frac{\beta^*\Lambda\eta_2}{K} & 0 \\ \xi\alpha_1 & -\mu & 0 & -\frac{\beta^*\Lambda\xi c_1\alpha_1}{\mu K} & -\frac{\beta^*\Lambda\eta_1\xi c_1\alpha_1}{\mu K} & -\frac{\beta^*\Lambda\eta_2\xi c_1\alpha_1}{\mu K} & 0 \\ \xi\alpha_2 & 0 & -\mu & -\frac{\beta^*\Lambda\xi c_2\alpha_2}{\mu K} & -\frac{\beta^*\Lambda\eta_1\xi c_2\alpha_2}{\mu K} & -\frac{\beta^*\Lambda\eta_2\xi c_2\alpha_2}{\mu K} & 0 \\ 0 & 0 & 0 & \frac{\beta^*\Lambda Q}{\mu K} - L & \frac{\beta^*\Lambda\eta_1 Q}{\mu K} & \frac{\beta^*\Lambda\eta_2 Q}{\mu K} & 0 \\ 0 & 0 & 0 & \theta & -M & 0 & 0 \\ 0 & 0 & 0 & 0 & \tau & -W & 0 \\ 0 & 0 & 0 & \sigma_1 & \sigma_2 & \sigma_3 & -P \end{pmatrix}. \tag{32}$$

The characteristic equation in (32), given by $|J(\mathcal{E}_0, \beta^*) - \lambda I| = 0$, gives a simple zero eigenvalues with other six eigenvalues having negative real part. The eigenvalues of the characteristic equation

are $\lambda_1 = \lambda_2 = -\mu$, $\lambda_3 = -K$, $\lambda_4 = -P$, $\lambda_5 = 0$ and the remaining eigenvalues are the solutions of the following characteristic equation

$$\lambda^2 + h_1\lambda + h_2 = 0, \tag{33}$$

with h_1, h_2 as in Equation (24). The Equation (33) has negative roots ($\lambda_6 < 0$, $\lambda_7 < 0$) when satisfies the discriminant $D = h_1^2 - 4h_2$ is positive, $\lambda_6.\lambda_7 = h_2 > 0$ and $\lambda_6 + \lambda_7 = h_1 < 0$.

Further, the right eigenvector associated with the zero eigenvalues is denoted by $w = (w_1, w_2, \cdots, w_7)^T$ can be obtained from $J(\mathcal{E}_0, \beta^*)w = 0$,

$$w_1 = -\frac{\Lambda\beta^* w_4(MW + W\eta_1\theta + \eta_2\tau\theta)}{K^2 MW}, \quad w_2 = -\frac{\Lambda\beta^*\xi\alpha_1 w_4(MW + W\eta_1\theta + \eta_2\tau\theta)(Kc_1 + \mu)}{u^2 K^2 MW}$$

$$w_3 = -\frac{\Lambda\beta^*\xi\alpha_2 w_4(MW + W\eta_1\theta + \eta_2\tau\theta)(Kc_2 + \mu)}{\mu^2 K^2 MW}, \quad w_4 = w_4, \quad w_5 = \frac{\theta w_4}{M}, \quad w_6 = \frac{\tau\theta w_4}{MW},$$

$$w_7 = \frac{w_4(MW\sigma_1 + W\sigma_2\theta + \sigma_3\tau\theta)}{MWP}.$$

Thus, it was chosen $w_4 > 0$ results in w_2, w_3, w_5, w_6, w_7 being positive. Moreover, the left eigenvector $v = (v_1, v_2, v_3, v_4, v_5, v_6, v_7)$ satisfying $v \cdot w = 1$ is given by

$$v_1 = 0, \ v_2 = 0, \ v_3 = 0, \ v_4 = \frac{1}{w_4}\left(\frac{\mu K M^2 W^2}{\mu K M^2 W^2 + \beta^*\theta\Lambda Q(W^2\eta_1 + \eta_2\tau W + \eta_2\tau M)}\right),$$

$$v_5 = \frac{v_4\beta^*\Lambda Q(W\eta_1 + \eta_2\tau)}{\mu K M W}, v_6 = \frac{v_4\beta^*\Lambda\eta_2 Q}{KW}, \ v_7 = 0.$$

According to Theorem 4.1 in [33], we calculate the bifurcation coefficient $\tilde{a}$ and $\tilde{b}$, we have

$$\tilde{a} = \sum_{k,i,j=1}^{7} v_k w_i w_j \frac{\partial^2 f_k(\mathcal{E}_0, \beta^*)}{\partial x_i \partial x_j}$$

$$= \frac{1}{K^3 M^4 W^4 \mu^3}\left\{2\beta^*\Lambda w_4\left(\beta^*\Lambda\eta_2\tau\theta(M+W) + \beta^*\Lambda W^2\eta_1\theta)Q + KM^2 W^2\mu\right)\right\}$$

$$\times\left(W\eta_1\theta + \eta_2\tau\theta + MW\right)B_0$$

and

$$\tilde{b} = \sum_{k,i=1}^{7} v_k w_i \frac{\partial^2 f_k(\mathcal{E}_0, \beta^*)}{\partial x_i \partial\beta} = v_4 w_4 \frac{\partial^2 f_4(\mathcal{E}_0, \beta^*)}{\partial x_4 \partial\beta} + v_4 w_5 \frac{\partial^2 f_4(\mathcal{E}_0, \beta^*)}{\partial x_5 \partial\beta} + v_4 w6 \frac{\partial^2 f_4(\mathcal{E}_0, \beta^*)}{\partial x_6 \partial\beta}$$

$$= \frac{\Lambda MQW\left(W\eta_1\theta + \eta_2\tau\theta + MW\right)}{\beta^*\Lambda Q\theta\left(M\eta_2\tau + W^2\eta_1 + W\eta_2\theta\right) + \mu K M^2 W^2},$$

where

$$B_0 = \left(K\beta^*\xi\left(\alpha_1 c_1\psi_1 + \alpha_2 c_2\psi_2\right) + \beta^*\mu\xi\left(\alpha_1 + \alpha_2\right)\right)\left(W\eta_1\theta + \eta_2\tau\theta + MW\right)$$

$$+ K\mu\omega\left(W\theta\xi + MW + \tau\theta\right)\left(\alpha_1\psi_1 + \alpha_2\psi_2\right)$$

$$-\left(K\beta^*\xi\left(\alpha_1 c_1 + \alpha_2 c_2\right) + \beta^*\mu\xi\left(\alpha_1\psi_1 + \alpha_2\psi_2\right) + \beta^*\mu^2\right)\left(W\eta_1\theta + MW + \eta_2\tau\theta\right)$$

$$- K\mu^2\omega\left(MW + W\theta + \tau\theta\right) - K\theta\xi\mu\omega\left(MW + \tau + W\right)\left(\alpha_1 + \alpha_2\right).$$

It is important to highlight that the coefficient $\tilde{b}$ is always positive. Consequently, the local dynamics around the disease-free equilibrium point are determined by the sign of the coefficient $\tilde{a}$. A backward bifurcation of system (8) occurs if $\tilde{a}$ is positive, whereas a forward bifurcation occurs if $\tilde{a}$ is negative. Alternatively, model (8) exhibits a forward bifurcation if $B_0 < 0$. Thus, the proof of Theorem 4 is completed. □

To demonstrate this phenomenon in relation to the above Theorem 4, the same parameter values used in Table 1 are used and forward bifurcation diagrams are depicted in Figure 2. For this set of parameter values, the associated forward bifurcation coefficient are $\tilde{a} = -513.753554$ with

$B_0 = -1.517129 \times 10^{-5}$ and $\tilde{b} = 13,433.84676$. The bifurcation parameter at the point where $\mathcal{R}_e = 1$ is $\beta^* = 1.389119 \times 10^{-5}$.
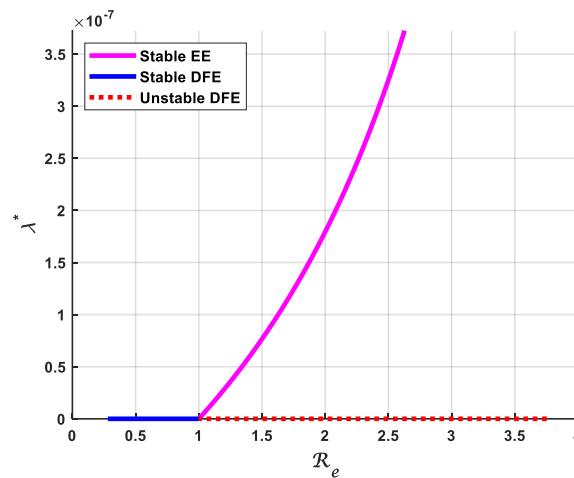

Figure 2. Plot of the forward bifurcation based on $\mathcal{R}_e$ versus λ^*..

Figure 2 illustrates the system's behaviour as the effective reproduction number $\mathcal{R}_e$ varies. When $\mathcal{R}_e < 1$, the disease-free equilibrium (DFE) $\mathcal{E}_0$ is locally asymptotically stable, as shown by the solid blue line. However, when $\mathcal{R}_e > 1$, the DFE $\mathcal{E}_0$ becomes unstable, indicated by the dashed blue line. The ascending magenta line in Figure 2 represents a stable endemic equilibrium (EE) $\mathcal{E}_1$, indicating a transition from the DFE to the EE, which suggests the sustained presence of the virus in the population.

For $\mathcal{R}_e > 1$, the applying Descartes' Rule of Signs, along with the conditions $a_3 > 0$ and $a_1 < 0$, the cubic polynomial in Equation (24), the number of positive real roots can be determined, as summarized in Table 2. In contrast, when $\mathcal{R}_e < 1$, no endemic equilibrium exists. Figure 2 depicts these equilibria, highlighting a forward bifurcation occurring at $\mathcal{R}_e = 1$. In the figure, the solid blue line represents the stable disease-free equilibrium $\mathcal{E}_0$ for $\mathcal{R}_e < 1$, while the dashed blue line shows the unstable DFE for $\mathcal{R}_e > 1$. The ascending magenta curve represents the stable branch of the endemic equilibrium $\mathcal{E}_1$. Consequently, $\mathcal{E}_1$ is stable when $\mathcal{R}_e > 1$ and unstable when $\mathcal{R}_e < 1$. Similarly, $\mathcal{E}_0$ is stable for $\mathcal{R}_e < 1$ and becomes unstable for $\mathcal{R}_e > 1$.

3.5. Sensitivity Analysis

The sensitivity analysis of model parameters is an important aspect of the present study. This analysis identifies the relevant sensitivity indices for each parameter, highlighting its role in the disease dynamics. In this section, we present a sensitivity analysis of various model parameters concerning the threshold quantity $\mathcal{R}_e$. Furthermore, this analysis helps to identify the parameters that have a significant influence on $\mathcal{R}_e$, making them potential targets for intervention. A parameter that has a significant impact on $\mathcal{R}_e$ indicates its dominant role in determining the endemicity of HIV/AIDS.

Following the methods described in [36], we perform the analysis by calculating the sensitivity indices of the model parameters. To conduct the sensitivity analysis, the normalized forward sensitivity index of a variable concerning a given parameter is determined. The sensitivity index of $\mathcal{R}_e$ concerning the parameter φ is defined by the following formula:

$$\Upsilon_\varphi^{\mathcal{R}_e} = \frac{\partial \mathcal{R}_e}{\partial \varphi} \frac{\varphi}{\mathcal{R}_e} .$$

(34)

A parameter with a larger sensitivity index value has greater influence than a parameter with a smaller sensitivity index value. The sign of the sensitivity indices $\mathcal{R}_e$ concerning a parameter indicates whether the parameter has a positive or negative effect on $\mathcal{R}_e$. Specifically, if the sign of the sensitivity indices is positive, then the value of $\mathcal{R}_e$ increases as the parameter increases; conversely, if the sign of the sensitivity indices is negative, then the value of $\mathcal{R}_e$ decreases as the parameter increases. The sensitivity indices of various model parameters, calculated using the expression given in (34), are presented in Table 2. The effective reproduction number of the model (8) depends on fifteen parameters, namely, $\Lambda, \beta, \mu, \theta, \psi_1, \psi_2, \xi, \sigma_1, \sigma_2, \sigma_3, \alpha_1, \alpha_2, \eta_1, \eta_2,$ and τ. Table 2 presents the sensitivity index values and ranks the parameters from most to least sensitive. Parameters $\beta, \Lambda, \eta_1,$ and η_2 with positive sensitivity indices indicate that the remaining parameters have negative sensitivity indices.

Figure 3 presents the sensitivity index values of various model parameters, calculated using expression (34), and arranged in descending order from the most sensitive to the least sensitive (left to right). An absolute value of the sensitive index greater than 0.5 is considered to have a significant effect on $\mathcal{R}_e$. The most sensitive parameter is the effect-contact rate (β) and with a sensitivity index value given by 1. This means that if the value of β is increased (decreased) by 10% while other parameter values are constant, the value of $\mathcal{R}_e$ increased (decreased) by 10%. Conversely, the sensitive index value of θ is -0.7716, indicating that increasing (decreasing) the value of θ while other parameter values are constant, will be followed by a decrease (increase) in the value of $\mathcal{R}_e$ by 7.716 %. The same interpretation applies to the other parameters.

Table 2. Sensitivity indices of R_e corresponding to the parameters of model (8).

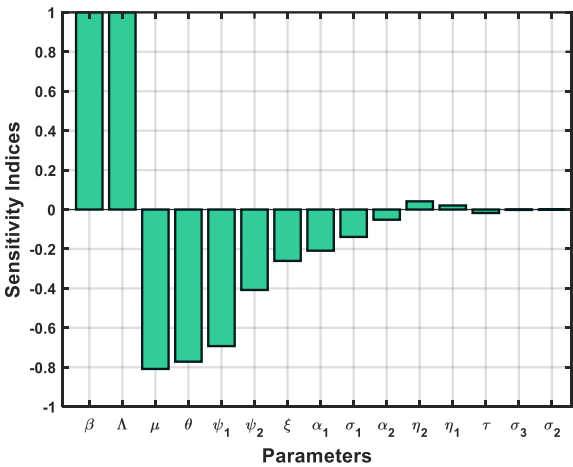| Parameter	Sensitivity Indices	Parameter	Sensitivity Indices
β	1	σ_1	-0.1389
Λ	0.9999	α_2	-0.0517
μ	-0.8083	η_2	0.0417
θ	-0.7716	η_1	0.0206
ψ_1	-0.6925	τ	-0.0176
ψ_2	-0.4079	σ_3	-0.0020
ξ	-0.2605	σ_2	-0.0009
α_1	-0.2088		

Figure 3. Bar plot of the sensitivity index of $\mathcal{R}_e$ with respect to each parameter.

We have illustrated the impact of several key parameters graphically in Figure 4. Figure 4(a) shows the effect of parameter β on the transmission dynamics of HIV. According to the graph, HIV infection is eradicated when the effective contact rate is reduced to 0.0000251. This demonstrates that

HIV transmission can be stopped by reducing the rate of contact between susceptible and infective individuals below this threshold.
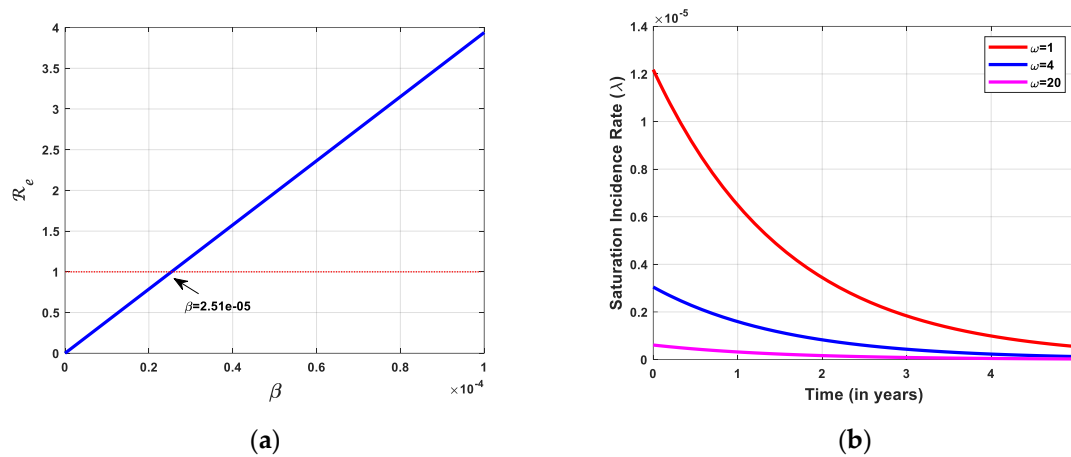

Figure 4. (a) The relationship among $\mathcal{R}_e$ and β; (b) Impact of inhibitory effect (ω) on the saturation incidence rate (λ).

The effects of increasing the saturation rate are evaluated through numerical simulations presented in Figure 4(b). The psychological or inhibitory effect (denoted by ω) is used to assess the influence of saturation, even though it does not directly affect the effective reproduction number. The numerical results indicate that the saturation rate decreases as the inhibitory effects increase.

4. Optimal Control Model

In this section, the deterministic model (8) is developed into a control problem by considering the parameters $\xi, \theta,$ and τ as continuous variables that depend on time. The optimal control parameters and conditions are considered as follows:

- The parameter u_1 $(0 \leq u_1 \leq 1)$ represents the proportion of the susceptible subpopulation that receives the educational campaign and adopts AB (Abstinence, Be faithful) and C (use Condoms) behaviours.
- The parameter u_2 $(0 \leq u_2 \leq 1)$ represents the proportion of the unaware infective subpopulation that receives screening per unit of time.
- The parameter u_3 $(0 \leq u_3 \leq 1)$ represents the proportion of the aware infective subpopulation that receives antiretroviral treatment per unit time.

The control variables $u_1, u_2,$ and u_3 are defined on the closed interval $[0, T_f]$, where T_f denotes the final time of the control implementations. By integrating the three previously described control strategies into the dynamic system (1), the corresponding system of differential equations is reformulated as follows:

$$\frac{dS}{dt} = \Lambda - \lambda(I_u, I_a, T)S - (u_1\alpha_1 + u_1\alpha_2 + \mu)S,$$

$$\frac{dE_1}{dt} = u_1\alpha_1 S - (1-\psi_1)\lambda(I_u, I_a, T)E_1 - \mu E_1,$$

$$\frac{dE_2}{dt} = u_1\alpha_2 S - (1-\psi_2)\lambda(I_u, I_a, T)E_2 - \mu E_2,$$

$$\frac{dI_u}{dt} = \lambda(I_u, I_a, T)S + (1-\psi_1)\lambda(I_u, I_a, T)E_1 + (1-\psi_2)\lambda(I_u, I_a, T)E_2 - (u_2 + \sigma_1 + \mu)I_u, \qquad (35)$$

$$\frac{dI_a}{dt} = u_2 I_u - (u_3 + \sigma_2 + \mu)I_a,$$

$$\frac{dT}{dt} = u_3 I_a - (\sigma_3 + \mu)T,$$

$$\frac{dA}{dt} = \sigma_1 I_u + \sigma_2 I_a + \sigma_3 T - (\gamma + \mu)A,$$

with the corresponding initial conditions are given in Equation (9).

4.1. Optimal Control Problem

In this section, we analyze the behaviour of the given model by using optimal control theory. The main objective is to minimizes the number of infected individuals (I_u and I_a) and the control costs associated with the educational campaigns (u_1), screening of the unaware infective subpopulation (u_2), and antiretroviral therapy for the aware infective subpopulation (u_3). The objective functional for a fixed time T_f, given by

$$J(u_1, u_2, u_3) = \int_0^{T_f} \left[B_1 I_u + B_2 I_a + \tfrac{1}{2}(C_1 u_1^2 + C_2 u_2^2 + C_3 u_3^2) \right] dt, \qquad (36)$$

where $B_1 \geq 0$, $B_2 \geq 0$ are nonnegative weight constant on the unaware and aware infected individuals, whereas C_i ($i = 1, 2, 3$) are the relative costs of the controls associated control u_i ($i = 1, 2, 3$).

The main goal of this part is to find the optimal control strategies $u^* = (u_1^*, u_2^*, u_3^*)$, subject to (35) and minimizing the objective functional Eq (36) such that

$$J(u_1^*, u_2^*, u_3^*) = \min\left\{ J(u_1, u_2, u_3) : u_1, u_2, u_3 \in U \right\} \qquad (37)$$

where $U = \left\{ (u_1, u_2, u_3) \in \mathbb{R}^3 : 0 \leq u_i \leq 1, i = 1, 2, 3, \ t \in [0, T_f] \right\}$ is the control set.

4.2. Existence of an Optimal Controls

This section investigates the existence of an optimal control triple that minimize the objective functional J defined in Equation (36). To establish this, we employ the existence theorem by Fleming and Rishel [37].

Theorem 5. *Given the objective functional J defined on the control set U, there exists an optimal control triple $u^* = (u_1^*, u_2^*, u_3^*)$ such that* Equation *(37) is satisfied, provided the five following conditions hold [37]:*

(i) The optimal control set, and state variables set are nonempty.

(ii) The control set U is closed and convex.

(iii) The right-hand side of the state system (35) is continuous and bounded by a linear function in both the state and control variables.

(iv) The integrand of the objective functional J in Equation *(36) is convex concerning the control set U.*

(v) There exist constants $d_1 > 0, d_2 > 0$, and $d_3 > 1$ such that the integrand of the objective functional J in (36) is bound below by

$$d_1 \left(\sum_{i=1}^{3} |u_i|^2 \right)^{d_3/2} - d_2 .$$

Proof. We must confirm the validity of the fife conditions specified in Theorem 5.

(i) Clearly, U is a nonempty set of measurable functions in $\mathbb{R}$, and the corresponding solutions exist and remain bounded.

(ii) Given the control set $U = \{u = (u_1, u_2, u_3) \epsilon \mathbb{R}^3 : 0 \le u_i \le 1, i = 1,2,3\}$. This set can be expressed as $U = U_1 \times U_2 \times U_3$, where each $U_i \subseteq [0,1]$, indicating U is bounded for all $t \in [0, T_f]$. Consequently, U is closed. Now, let $a = (a_1, a_2, a_3)$ and $b = (b_1, b_2, b_3)$ any two arbitrary elements in U. By the definition of a convex set [38], it follows that $\varphi a_j + (1-\varphi) b_j \in [0,1]$ for all $j = 1, 2, 3$. Hence, $\varphi a + (1-\varphi) b \in U$, which implies that U is a convex set.

(iii) Let $x = (S, E_1, E_2, I_u, I_a, T, A)$ be the state variables of the model (8) and $(u_1, u_2, u_3) \in U$. Then the right-hand side of the system (35) can be written as $g(t, x, u) = g_1(t, x) + g_2(t, x)u$, where

$$g(t, x, u) = \begin{pmatrix} \Lambda - \lambda(I_u, I_a, T)S - (u_1\alpha_1 + u_2\alpha_2 + \mu)S \\ u_1\alpha_1 S - \lambda(I_u, I_a, T)c_1 E_1 - \mu E_1 \\ u_1\alpha_2 S - \lambda(I_u, I_a, T)c_2 E_2 - \mu E_2 \\ \lambda(I_u, I_a, T)(S + c_1 E_1 + c_2 E_2) - (u_2 + \sigma_1 + \mu)I_u \\ u_2 I_u - (u_3 + \sigma_2 + \mu)I_a \\ u_3 I_a - WT \\ \sigma_1 I_u + \sigma_2 I_a + \sigma_3 T - PA \end{pmatrix},$$

$$g_1(t, x) = \begin{pmatrix} \Lambda - \lambda(I_u, I_a, T)S - \mu S \\ -\lambda(I_u, I_a, T)c_1 E_1 - \mu E_1 \\ -\lambda(I_u, I_a, T)c_2 E_2 - \mu E_2 \\ \lambda(I_u, I_a, T)(S + c_1 E_1 + c_2 E_2) - (\sigma_1 + \mu)I_u \\ -(\sigma_2 + \mu)I_a \\ -WT \\ \sigma_1 I_u + \sigma_2 I_a + \sigma_3 T - PA \end{pmatrix}, \quad g_2(t, x) = \begin{pmatrix} -\alpha_1 S & -\alpha_2 S & 0 \\ \alpha_1 S & 0 & 0 \\ \alpha_2 S & 0 & 0 \\ 0 & -I_u & 0 \\ 0 & I_u & -I_a \\ 0 & 0 & I_a \\ 0 & 0 & 0 \end{pmatrix}.$$

Derived from the Euclidean norm of a matrix as indicated in [26,28], we obtain $\|g(t, x, u)\| = \|g_1(t, x)\| + \|g_2(t, x)\| \|u\|$. This means that the right-hand side of the model (8) can be expressed as a linear function of the controls u_1, u_2, and u_3 with coefficients depending on state variables.

(iv) The integrand of the objective functional (36) can be expressed in the form of a Lagrangian as $\mathcal{L} = B_1 I_u + B_2 I_a + \frac{1}{2}(C_1 u_1^2 + C_2 u_2^2 + C_3 u_3^2) = h_1(t, x) + h_2(t, u)$. To establish convexity, it is sufficient to show that the term $h_2(t, u) = \frac{1}{2}\sum_{i=1}^{3} C_i u_i^2$ is convex on the control set U. Notice that $h_2(t, u)$ is formed as a finite linear sum of the functions $q_i = \frac{1}{2}u_i^2$. Therefore, it is easier to show that the function $q: U \to \mathbb{R}$ given by $q = \frac{1}{2}u^2$ is convex. Let $y, z \in U$ and $\phi \in [0, 1]$. Then,

$$q(\phi y + (1-\phi)z) - (\phi q(y) + (1-\phi)q(z)) = \frac{1}{2}(\phi y + (1-\phi)z)^2 - \frac{1}{2}(\phi y^2 + (1-\phi)z^2)$$

$$= \frac{1}{2}(\phi^2 - \phi)(y - z)^2 \le 0, \text{ since } \phi \in [0, 1].$$

Hence, $q(\phi y + (1-\phi)z) \le (\phi q(y) + (1-\phi)q(z))$. Thus, the condition satisfies the definition of a convex function as stated in [45]. As a result, the function $h_2(t, u)$ is convex function on U.

(v) By applying the Lagrangian equation $\mathcal{L}$, we demonstrate the final condition as follows:

$$\mathcal{L} = B_1 I_u + B_2 I_a + \tfrac{1}{2}\left(C_1 u_1^2 + C_2 u_2^2 + C_3 u_3^2\right) \geq \tfrac{1}{2}\left(C_1 u_1^2 + C_2 u_2^2 + C_3 u_3^2\right)$$

$$\geq \min\left\{\tfrac{1}{2}C_1, \tfrac{1}{2}C_2, \tfrac{1}{2}C_3\right\}\left(\sum_{i=1}^{3} u_i^2\right)^{\frac{2}{2}} - C_2 \geq d_1\left(\sum_{i=1}^{3}|u_i|^2\right)^{\frac{d_3}{2}} - d_2,$$

where $d_1 = \min\left\{\tfrac{1}{2}C_1, \tfrac{1}{2}C_2, \tfrac{1}{2}C_3\right\}, d_3 = 2,$ and $d_2 = C_2 > 0$.

The proof of Theorem 5 is completed. □

4.3. Characterization of the Optimal Control

We characterize the optimal control triple $u^* = (u_1^*, u_2^*, u_3^*)$ of the system and the corresponding states $x^* = (S^*, E_1^*, E_2^*, I_u^*, I_a^*, T^*, A^*)$ with its control function $u_1, u_2,$ and u_3, with the objective functional Equation (36). Using Pontryagin's Maximal Principle [8,9], we obtain the necessary conditions for the optimal controls. Pontryagin's Maximal Principle convert Equation (35) and Equation (37) into a problem of minimizing pointwise a Hamiltonian, $\mathcal{H}$ concerning $u_1, u_2,$ and u_3. The Hamiltonian $\mathcal{H}$ is defined as follows:

$$\begin{aligned}
\mathcal{H} &= B_1 I_u + B_2 I_a + \tfrac{1}{2}(C_1 u_1^2 + C_2 u_2^2 + C_3 u_3^2) + \lambda_1\left(\Lambda - \lambda(I_u, I_a, T)S - u_1(\alpha_1 + \alpha_2)S - \mu S\right) \\
&+ \lambda_2\left(u_1\alpha_1 S - (1-\psi_1)\lambda(I_u, I_a, T)E_1 - \mu E_1\right) + \lambda_3\left(u_1\alpha_2 S - (1-\psi_2)\lambda(I_u, I_a, T)E_2 - \mu E_2\right) \\
&+ \lambda_4\left(\lambda(I_u, I_a, T)S + 1 - \psi_1)\lambda(I_u, I_a, T)E_1 + 1 - \psi_2)\lambda(I_u, I_a, T)E_2 - (u_2 + \sigma_1 + \mu)I_u\right) \\
&+ \lambda_5\left(u_2 I_u - (u_3 + \sigma_2 + \mu)I_a\right) + \lambda_6\left(u_3 I_a - (\sigma_3 + \mu)\right) + \lambda_7\left(\sigma_1 I_u + \sigma_2 I_a + \sigma_3 T - (\gamma + \mu)A\right).
\end{aligned} \tag{38}$$

where $\lambda_1, \lambda_2, \lambda_3, \lambda_4, \lambda_5, \lambda_6,$ and λ_7 are the adjoint variables.

The following result gives the necessary conditions for the optimal control.

Theorem 6. *Given an optimal controls (u_1^*, u_2^*, u_3^*) that minimizes the objective functional J over the control set U subject to system (1), then there exist the adjoint variables $\lambda_1, \lambda_2, \lambda_3, \lambda_4, \lambda_5, \lambda_6,$ and λ_7 satisfying the following equations:*

$$\frac{d\lambda_1}{dt} = (\lambda_1 - \lambda_4)\frac{\beta(I_u + \eta_1 I_a + \eta_2 T)S}{1 + \omega(I_u + I_2 + T)} + (\lambda_1 - \lambda_2)u_1\alpha_1 + (\lambda_1 - \lambda_3)u_1\alpha_2 + \lambda_1\mu,$$

$$\frac{d\lambda_2}{dt} = (\lambda_2 - \lambda_4)\frac{c_1\beta(I_u + \eta_1 I_a + \eta_2 T)S}{1 + \omega(I_u + I_2 + T)} + \lambda_2\mu,$$

$$\frac{d\lambda_3}{dt} = (\lambda_3 - \lambda_4)\frac{c_2\beta(I_u + \eta_1 I_a + \eta_2 T)S}{1 + \omega(I_u + I_2 + T)} + \lambda_3\mu,$$

$$\begin{aligned}
\frac{d\lambda_4}{dt} &= -B_1 + (\lambda_1 - \lambda_4)\left(\frac{\beta S}{1 + \omega(I_u + I_2 + T)} - \frac{\beta(I_u + \eta_1 I_a + \eta_2 T)S\omega}{(1 + \omega(I_u + I_2 + T))^2}\right) + (\lambda_2 - \lambda_4)\left(\frac{c_1\beta E_1}{1 + \omega(I_u + I_2 + T)} - \frac{c_1\beta(I_u + \eta_1 I_a + \eta_2 T)E_1\omega}{(1 + \omega(I_u + I_2 + T))^2}\right) \\
&+ (\lambda_3 - \lambda_4)\left(\frac{c_2\beta E_2}{1 + \omega(I_u + I_2 + T)} - \frac{c_2\beta(I_u + \eta_1 I_a + \eta_2 T)E_2\omega}{(1 + \omega(I_u + I_2 + T))^2}\right) + (\lambda_4 - \lambda_7)\sigma_1 + (\lambda_4 - \lambda_5)u_2 + \lambda_4\mu,
\end{aligned}$$

$$\begin{aligned}
\frac{d\lambda_5}{dt} &= -B_2 + (\lambda_1 - \lambda_4)\left(\frac{\beta\eta_1 S}{1 + \omega(I_u + I_2 + T)} - \frac{\beta(I_u + \eta_1 I_a + \eta_2 T)S\omega}{(1 + \omega(I_u + I_2 + T))^2}\right) + (\lambda_2 - \lambda_4)\left(\frac{c_1\beta\eta_1 E_1}{1 + \omega(I_u + I_2 + T)} - \frac{c_1\beta(I_u + \eta_1 I_a + \eta_2 T)E_1\omega}{(1 + \omega(I_u + I_2 + T))^2}\right) \\
&+ (\lambda_3 - \lambda_4)\left(\frac{c_2\beta\eta_1 E_2}{1 + \omega(I_u + I_2 + T)} - \frac{c_2\beta(I_u + \eta_1 I_a + \eta_2 T)E_2\omega}{(1 + \omega(I_u + I_2 + T))^2}\right) + (\lambda_5 - \lambda_6)u_3 + (\lambda_5 - \lambda_7)\sigma_2 + \lambda_5\mu,
\end{aligned}$$

$$\begin{aligned}
\frac{d\lambda_6}{dt} &= (\lambda_1 - \lambda_4)\left(\frac{\beta\eta_2 S}{1 + \omega(I_u + I_2 + T)} - \frac{\beta(I_u + \eta_1 I_a + \eta_2 T)S\omega}{(1 + \omega(I_u + I_2 + T))^2}\right) + (\lambda_2 - \lambda_4)\left(\frac{c_1\beta\eta_2 E_1}{1 + \omega(I_u + I_2 + T)} - \frac{c_1\beta(I_u + \eta_1 I_a + \eta_2 T)E_1\omega}{(1 + \omega(I_u + I_2 + T))^2}\right) \\
&+ (\lambda_3 - \lambda_4)\left(\frac{c_2\beta\eta_2 E_2}{1 + \omega(I_u + I_2 + T)} - \frac{c_2\beta(I_u + \eta_1 I_a + \eta_2 T)E_2\omega}{(1 + \omega(I_u + I_2 + T))^2}\right) + (\lambda_6 - \lambda_7)\sigma_3 + \lambda_6\mu,
\end{aligned}$$

$$\frac{d\lambda_7}{dt} = (\lambda_7 - \lambda_6)\delta + (\gamma + \mu)\lambda_7. \tag{39}$$

with transversality conditions,

$$\lambda_j(T_f) = 0, \; j = 1, 2, 3, 4, 5, 6, 7.$$

Furthermore, the optimal, denoted as $u^* = (u_1^*, u_2^*, u_3^*)$ is expressed as follows:

$$u_1^* = \min\left\{\max\left(0, \frac{\left((\lambda_1 - \lambda_2)\alpha_1 + (\lambda_1 - \lambda_3)\alpha_2\right)S^*}{C_1}\right), 1\right\},$$

$$u_2^* = \min\left\{\max\left(0, \frac{(\lambda_4 - \lambda_5)I_u^*}{C_2}\right), 1\right\}, \tag{40}$$

$$u_3^* = \min\left\{\max\left(0, \frac{(\lambda_5 - \lambda_6)I_a^*}{C_3}\right), 1\right\}.$$

Proof. We apply Pontryagin's Maximum Principle to derive the adjoint variables, the transversality conditions, and the optimal control triplet. The system of adjoint equations (39) is obtained by taking the partial derivatives of the Hamiltonian in Equation (38) with respect to the corresponding state variables, $S, E_1, E_2, I_u, I_a, T, A$, as follows:

$$\frac{\partial \lambda_1}{\partial t} = -\frac{\partial \mathcal{H}}{\partial S}, \quad \lambda_1(T_f) = 0; \quad \frac{\partial \lambda_2}{\partial t} = -\frac{\partial \mathcal{H}}{\partial E_1}, \quad \lambda_2(T_f) = 0; \quad \frac{\partial \lambda_3}{\partial t} = -\frac{\partial \mathcal{H}}{\partial E_2}, \quad \lambda_3(T_f) = 0;$$

$$\frac{\partial \lambda_4}{\partial t} = -\frac{\partial \mathcal{H}}{\partial I_u}, \quad \lambda_4(T_f) = 0; \quad \frac{\partial \lambda_5}{\partial t} = -\frac{\partial \mathcal{H}}{\partial I_a}, \quad \lambda_5(T_f) = 0; \quad \frac{\partial \lambda_6}{\partial t} = -\frac{\partial \mathcal{H}}{\partial T}, \quad \lambda_6(T_f) = 0;$$

$$\frac{\partial \lambda_7}{\partial t} = -\frac{\partial \mathcal{H}}{\partial A}, \quad \lambda_7(T_f) = 0.$$

Finally, the optimal controls can be characterized from $\mathcal{H}$ in Equation (38) by applying the optimality conditions for each control measure u_i, where $0 \le u_i \le 1$, for $i = 1, 2, 3$. Thus,

$$\frac{\partial \mathcal{H}}{\partial u_1} = 0, \quad \frac{\partial \mathcal{H}}{\partial u_1} = 0, \quad \frac{\partial \mathcal{H}}{\partial u_1} = 0. \tag{41}$$

By solving Equation (41) with the optimal controls u_1^*, u_2^*, and u_3^*, we derive the following characterization:

$$\tilde{u}_1 = \frac{\left((\lambda_1 - \lambda_2)\alpha_1 + (\lambda_1 - \lambda_3)\alpha_2\right)S^*}{C_1}, \quad \tilde{u}_2 = \frac{(\lambda_4 - \lambda_5)I_u^*}{C_2}, \quad \tilde{u}_3 = \frac{(\lambda_5 - \lambda_6)I_a^*}{C_3}. \tag{42}$$

Since all three control measures are bounded between 0 and 1, we have

$$u_i^* = \begin{cases} 0 & \text{if} \quad \tilde{u}_i^* \le 0, \\ \tilde{u}_i^* & \text{if} \quad 0 < \tilde{u}_i^* < 1, \\ 1 & \text{if} \quad \tilde{u}_i^* \ge 1. \end{cases}$$

where

$$\tilde{u}_1 = \frac{\left((\lambda_1 - \lambda_2)\alpha_1 + (\lambda_1 - \lambda_3)\alpha_2\right)S^*}{C_1}, \quad \tilde{u}_2 = \frac{(\lambda_4 - \lambda_5)I_u^*}{C_2}, \quad \tilde{u}_3 = \frac{(\lambda_5 - \lambda_6)I_a^*}{C_3}.$$

Hence, for these controls u_1^*, u_2^*, and u_3^* given in the Equation (40) are characterized by

$$u_1^* = \min\left\{\max\left(0, \tilde{u}_1\right), 1\right\}, u_2^* = \min\left\{\max\left(0, \tilde{u}_2\right), 1\right\}, u_3^* = \min\left\{\max\left(0, \tilde{u}_3\right), 1\right\}.$$

The proof of Theorem 6 is complete.   □

5. Numerical Simulations and Cost-Effectiveness Analysis

5.1. Numerical Simulation of Model

In this section, we present several numerical simulations of the model (8) to illustrate the dynamics of HIV transmission, using the parameter values estimated and shown in Table 2. These results aim to explore the dynamic effects of education, screening, and therapy interventions on HIV

incidence. To perform the simulations, both models are solved numerically using the fourth-order Runge-Kutta method and implemented in MATLAB. We set the initial population as follows:

$$\left(S(0), E_1(0), E_2(0), I_u(0), I_a(0), T(0), A(0)\right) = \left(2904903, 5000, 2500, 2408, 5390, 519, 1024\right). \quad (43)$$

First, we set parameter value $\beta = 0.00001$ and the other parameters as given in Table 1. We obtain $\mathcal{R}_e = 0.719881 < 1$. Theorem 1 is numerically illustrated in Figure 5, demonstrating the global stability of the DFE $\mathcal{E}_0 = (24154.59, 67287.79, 49541.66, 0, 0, 0, 0)$ within its region of attraction in both the $S - E_1 - I_a$ and $A - T - I_u$ spaces. Figure 5(a) shows that all solution trajectories starting within the area of attraction converge to the point $(S^0, E_1^0, I_a^0) = (24154.59, 67287.79, 0)$. Similarly, Figure 5(b) indicates that all trajectories originating within the region of attraction tend toward the point $(A^0, T, I_u^0) = (0, 0, 0)$. Three different initial values are used in constructing the stability diagram of $\mathcal{E}_0$ in three different state spaces, as follows: $N_1(20000, 40000, 30000, 2000, 1500, 1000, 1000)$, $N_2(22000, 42000, 32000, 2500, 2000, 2000, 1000)$, $N_3(24000, 44000, 34000, 3000, 2500, 2500, 2000)$, and $N_4 (25000, 45000, 35000, 3500, 3000, 3000, 2500)$. This approach can also be extended to demonstrate the global asymptotic stability of the disease-free equilibrium $\mathcal{E}_0$ in other subspaces of the model.

Second, we set parameter value $\beta = 0.00004$ while the remaining parameters are taken from Table 1. This results in the effective reproduction number of $\mathcal{R}_e = 2.879523 > 1$. Theorem 2 is numerically illustrated in Figure 6, demonstrating the global stability of the endemic equilibrium $\mathcal{E}_1 = (24151.41, 44846.37, 33015.99, 0.68, 0.64, 10.31, 0.24)$ within its region of attraction in both the $S - E_1 - I_a$ and $T - I_a - A$ spaces. In Figure 6(a), all solution trajectories that begin within the region of attraction $N_1, N_2, N_3,$ and N_4 converge to the point $(S^0, E_1^0, I_a^0) = (24151.41, 44846.37, 0)$. Figure 6(b) indicates that all trajectories that begin within the region of attraction tend toward the point $(T, I_a^0, A^0) = (10.31, 0.64, 0.24)$. This methodology can further be applied to verify the global asymptotic stability of the endemic equilibrium $\mathcal{E}_1$ in other subspaces of the model.
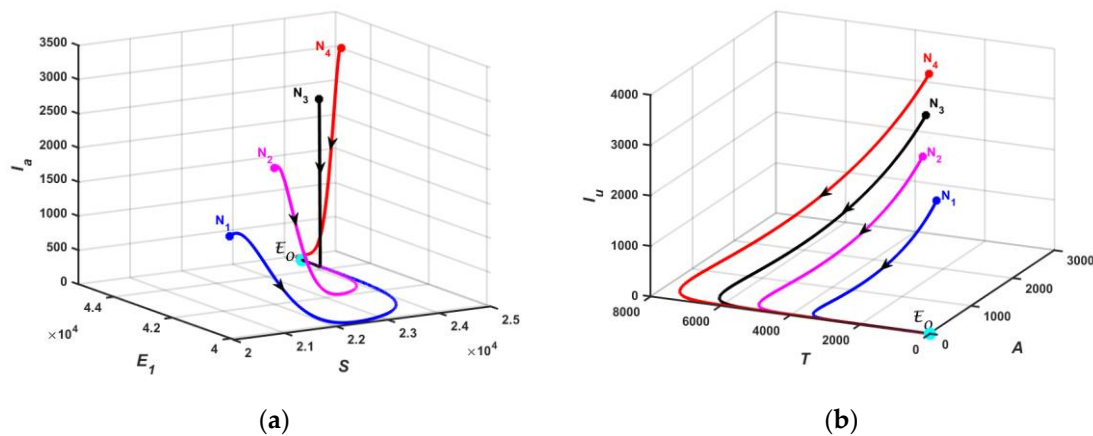

(a)   (b)

Figure 5. Globally asymptotically stable of the DFE $\mathcal{E}_0$ of model (8) in: (a) $\boldsymbol{S - E_1 - I_a}$ spaces; (b) $\boldsymbol{T - I_a - A}$ spaces.

Figure 6. Globally asymptotically stable of the EE $\mathcal{E}_1$ of model (8) in: (**a**) $S - E_1 - I_a$ spaces; (**b**) $T - I_a - A$ spaces.
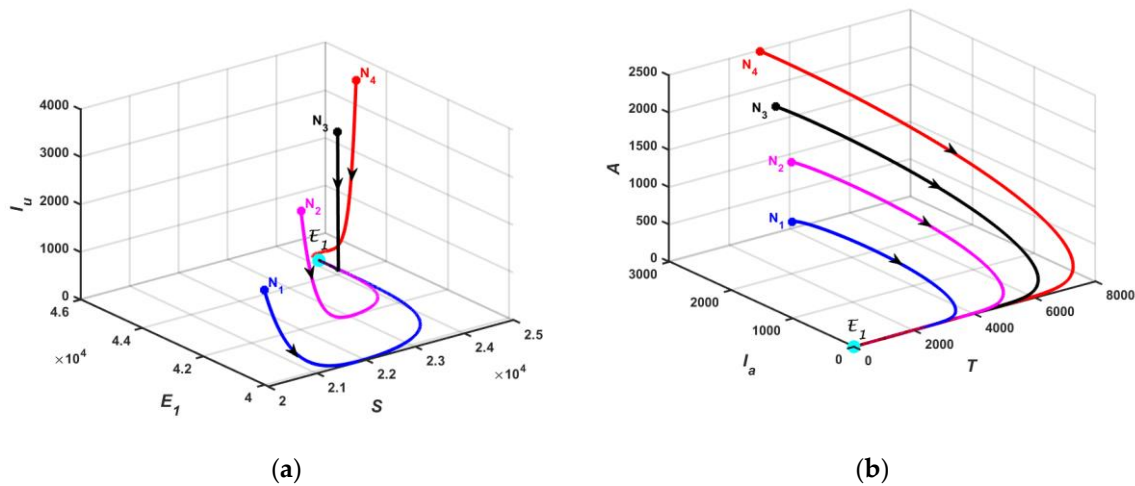
5.2. Optimal Control Simulation

We compute the numerical solution to the optimal control problem by solving the optimality system, which consists of the state and adjoint equations, using the forward-backward sweep method. This involves numerical integration using the fourth-order Runge-Kutta method implemented in MATLAB. Initially, the state system (35) is solved forward in time, with initial values determined by the transversality condition. Subsequently, the adjoint system (39) is solved backwards in time, utilizing the current iteration of state variables. The control variables are updated through a convex combination of their previous values and the new estimate derived from Equation (40). This iterative process is repeated until convergence of the state equations is achieved [18].

For numerical simulation purposes, the weight factors $B_1 = 1$ and $B_2 = 1$ are utilized, alongside cost coefficients $C_1 = 20, C_2 = 55$, and $C_3 = 75$. Simulations were conducted over a period of 5 years. These cost values are determined based on the efforts to implement the strategies under consideration. The parameter values presented in Table 1 and $\beta = 0.00004$ are employed in the simulations for cases where $\mathcal{R}_e = 2.879523 > 1$. To assess the impact of various optimal control strategies on the spread of HIV infection within the community, we will examine and compare the numerical results of interventions that implement multiple strategies. Strategies involving a single intervention are excluded, as they do not ensure the complete eradication of the disease from the community. This study considers the following four combined intervention strategies:

- Strategy A: Educational campaign combined with screening $(u_1 \neq 0, u_2 \neq 0, u_3 \neq 0)$.
- Strategy B: Educational campaign combined with treatment $(u_1 \neq 0, u_2 \neq 0, u_3 = 0)$.
- Strategy C: Screening combined with treatment $(u_1 \neq 0, u_2 = 0, u_3 \neq 0)$.
- Strategy D: Implementation of all control $(u_1 = 0, u_2 \neq 0, u_3 \neq 0)$.

5.2.1. Simulation for Strategi A $(u_1 \neq 0, u_2 \neq 0, u_3 \neq 0)$.

By implementing the triple control strategies simultaneously, we observed that Strategy A, which involves the simultaneous implementation of educational campaign control (u_1), screening control (u_2), and antiretroviral treatment control (u_3), significantly reduces the number of infected individuals (Figure 7). Specifically, at the final time ($T_f = 5$ years), the total number of unaware infectives under control is 36.7, compared to 1351.2 without control (Figure 7(a)). Similarly, the total number of aware infectives at time T_f is reduced to 105.36 with control, whereas it reaches 4648.5 in the absence control, which is significantly different (Figure 7(b)). Additionally, the total number of individuals with AIDS at time T_f is reduced to 269.8 with control, whereas it reaches 693.5 in the absence of control. These results demonstrate that the optimal control strategy is highly effective for
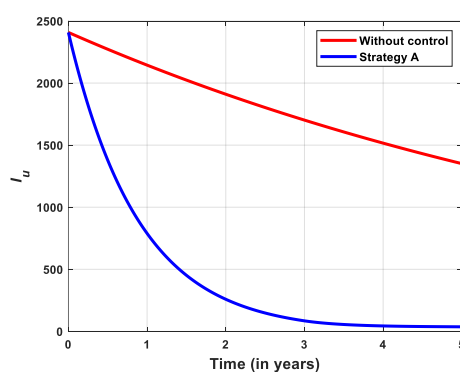
both groups of HIV-infected individuals and AIDS cases. Furthermore, Figure 7(d) illustrates the control profiles for Strategy A over time. To minimize the number of HIV infections and associated costs, the control u_1 is maintained at its upper limit for approximately 2.98 years before gradually decreasing to zero at the end of the control period. Similarly, the controls u_2 and u_3 are kept at their upper limit for 2.98 years and 4.35 years, respectively, before dropping to their lower bounds at the end of the control period.

5.2.2. Simulation for Strategi B

This strategy implements both intervention measures u_1(educational campaign control) and u_2 (screening controls). It is observed from Figure 8(a) to 8(c) that due to this control strategy, the number of unaware infectives, aware infectives, and AIDS individuals decreased only slightly during the control period. This result shows that the Strategy B has no significant effect on the subpopulation of the unaware infected individuals, aware infected individuals, and AIDS individuals. The control profile for the educational campaigns control u_1 at the beginning of the control period is at 0.53, then gradually decreases to zero at the end of the control period, while the control profile for screening control u_2 is maintained at its lower bound for the whole period (Figure 8(d)) .

5.2.3. Simulation for Strategi C

The simultaneous implementation of double control strategies demonstrates that Strategy C (i.e., applying educational campaign control and antiretroviral treatment) significantly reduces the number of infected individuals (Figure 9). Specifically, at the final time, the total number of unaware infectives under control is 9.7, compared to 1351.2 without control (Figure 9(a)). Similarly, the total number of aware infectives at time 5 years is reduced to 118.2 with control, whereas it reaches 4648.5 in the absence control, which is significantly different (Figure 9(b)). Additionally, at the final time, applying Strategy C leads to a significant decrease in the number of AIDS individuals (267.6) compared to the uncontrolled case (Figure 9(c)). Furthermore, Figure 9(d) illustrates the control profiles for Strategy C over time. The control profiles for the educational campaigns control u_1 at the beginning of the control period; it is at 0.09 then gradually decreases to zero at the end of the control period. The control profiles for the antiretroviral treatment control u_3 should be maintained at it upper bound for the first 4.4 years. After which both controls gradually decrease to it lower bound at the end of the period (Figure 9(d)). The optimal control profiles for u_1 and u_3 in Strategy C are identical to those in Strategy A.
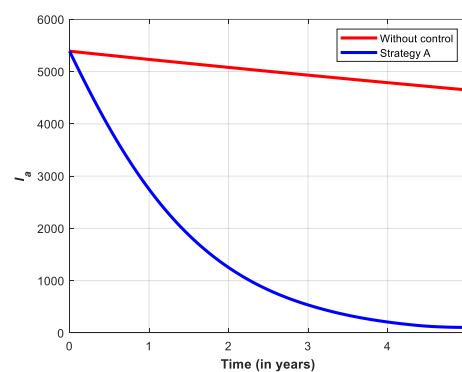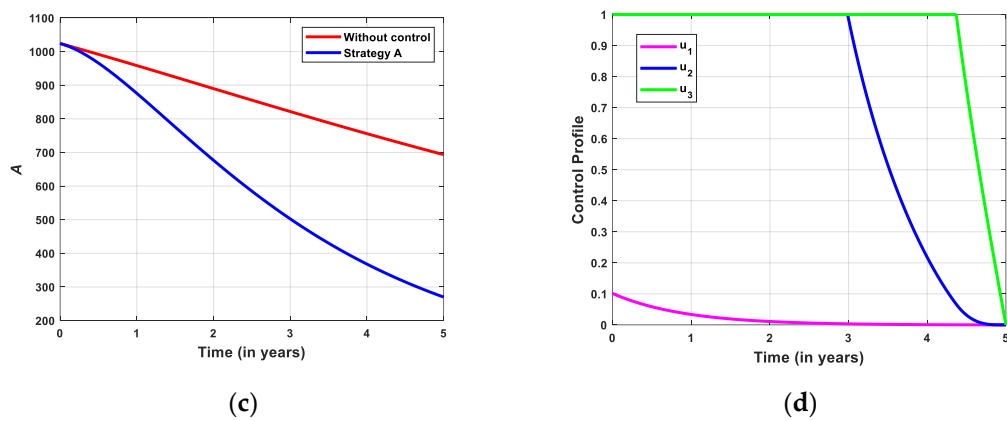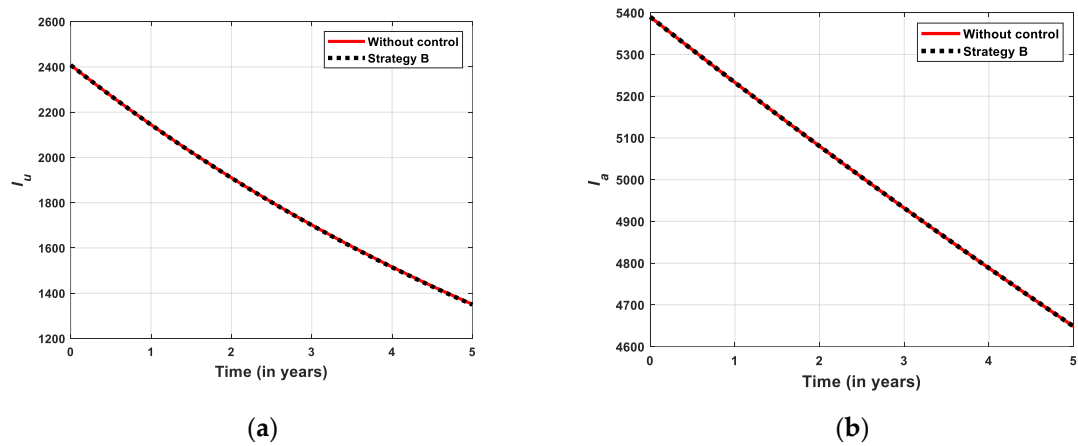

(**a**)   (**b**)

Figure 7. Simulation of the without control and with Strategy A on: (**a**) the number of I_u; (**b**) the number of I_a; (**c**) the number of A; (**d**) control profile of u_1, u_2, and u_3.

5.2.3. Simulation for Strategi C

The simultaneous implementation of double control strategies demonstrates that Strategy C (i.e., applying educational campaign control and antiretroviral treatment) significantly reduces the number of infected individuals (Figure 8). Specifically, at the final time, the total number of unaware infectives under control is 9.7, compared to 1351.2 without control (Figure 8(a)). Similarly, the total number of aware infectives at time 5 years is reduced to 118.2 with control, whereas it reaches 4648.5 in the absence control which is significantly different (Figure 9(b). Additionally, at the final time, applying Strategy C leads to a significant in the number of AIDS individuals (267.6) compared to the uncontrolled case (Figure 9(c)). The control profiles for the educational campaigns control u_1 at the beginning of the control period it is at 0.09 then gradually decreases to zero at the end of the control period. The control profiles for the antiretroviral treatment control u_3 should be maintained at its upper bound for the first 4.4 years. After which both controls gradually decrease to its lower bound at the end of the period (Figure 9(d)). The optimal control profiles for u_1 and u_3 in Strategy C are identical to those in Strategy A.
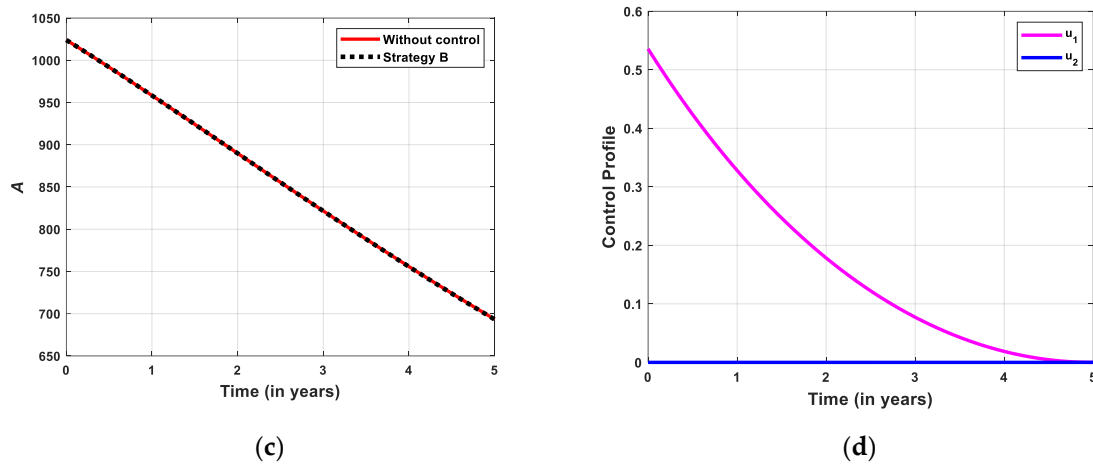
(**c**)   (**d**)

Figure 8. Simulation of the without control and with Strategy B on: (**a**) the number of I_u; (**b**) the number of I_a; (**c**) the number of A; (**d**) control profile of u_1 and u_2.

5.2.4. Simulation for Strategi D

This strategy implements both intervention measures u_2 (screening control) and u_3 (antiretroviral treatment). Specifically, at the final time (5 years), the total number of unaware infectives under control is 36.7, compared to 1351.2 without control (Figure 10(a)). Similarly, the total number of aware infectives at time T_f is reduced to 105.3 with control, whereas it reaches 4648.5 in the absence control, which is significantly different (Figure 10(b)). Additionally, at the final time, applying Strategy A leads to a significant decrease in the number of AIDS individuals (269.8) compared to the uncontrolled case (Figure 10(c)). The control profiles for the screening control u_2 should be maintained at it upper bound for the first 2.98 years, while the control profile for the antiretroviral treatment control (u_3) should be maintained at it upper bound for the first 4.36 years. After which both controls gradually decrease to it lower bound at the end of the period. The optimal control profiles for u_2 and u_3 in Strategy D are identical to those in Strategy A.

5.3. Cost-Effectiveness Analysis

To determine which control strategy is most effective, this subsection evaluates the economic implications of educational campaign strategies for susceptible individuals, screening for unaware infectives, and antiretroviral therapy for aware infectives in the dynamics of HIV/AIDS, using cost-effectiveness analysis (CEA). CEA helps identify and propose the most efficient or cost-effective strategy for implementation under limited sources. In this study, the evaluation will be conducted using the incremental cost-effectiveness ratio (ICER), which compares the difference in costs and health outcomes between two competing intervention strategies. Each intervention is compared to the next less effective alternative in terms of the number of infections averted [9]. When comparing two competing intervention strategies, p and q, The ICER is defined as follows [21,25].

$$\text{ICER} = \frac{\text{Change in total costs associated with strategies } p \text{ and } q}{\text{Change in control benefits obtained by implementing the strategies } p \text{ and } q} \cdot \text{(44)}$$

The total averted infections, used in the cost-effectiveness analysis table, is determined by the difference between the total number of infected individuals without any control and the total number with the implementation of a control strategy. The total cost associated with a control strategy is directly proportional to the number of controls applied. In this study, the ICER values were computed using formula (31). Specifically, the total cost (TC) and total averted infections (TA) for each strategy i were calculated using the following formulas:

$$TC(i) = \int_{i=1}^{T_f} \left[w_3 (u_1^*(t))^2 + w_4 (u_2^*(t))^2 + w_5 (u_3^*(t))^2 \right] dt , \qquad (45)$$

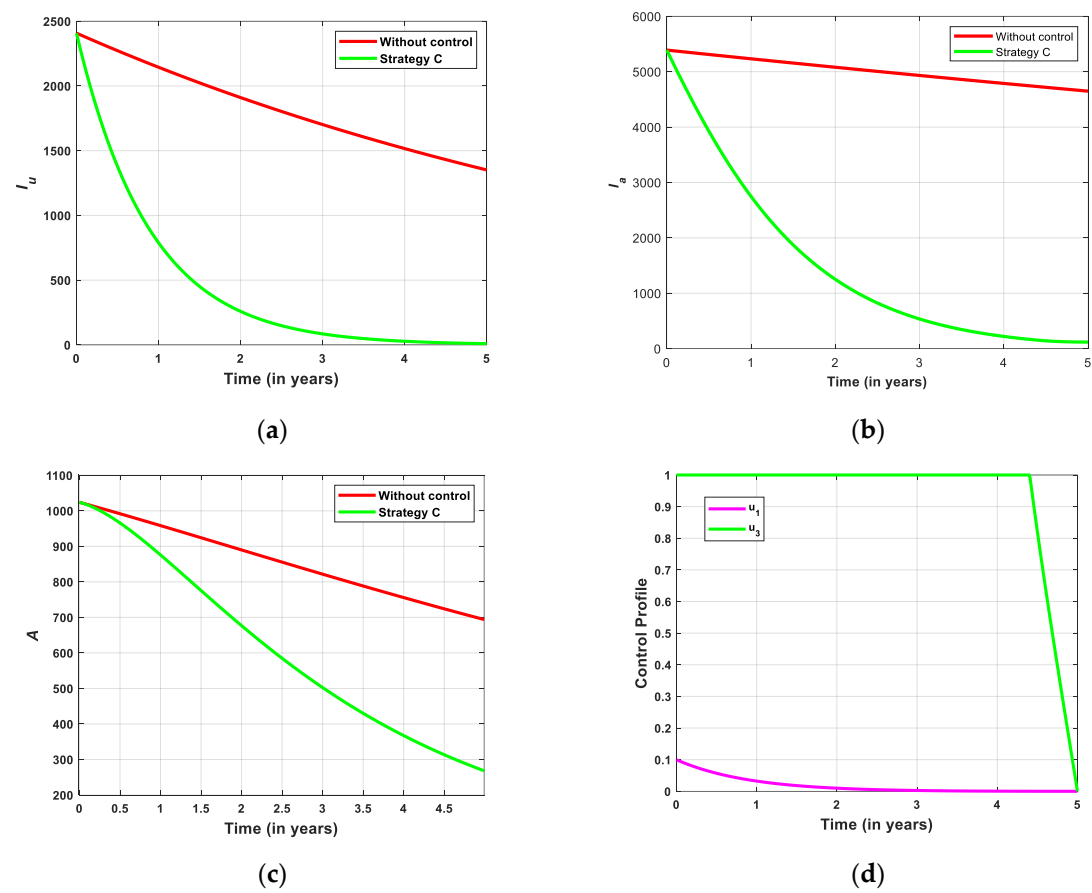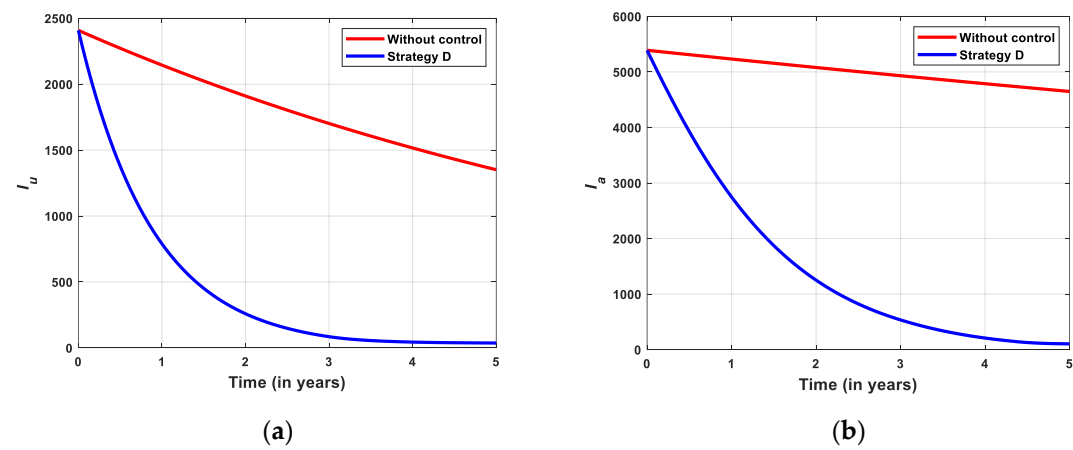$$TA(i) = \int_{i=1}^{T_f} \left[(I_u(t) - I_u^*(t)) + (I_a(t) - I_a^*(t)) + (A(t) - A^*(t)) \right] dt \, . \tag{46}$$
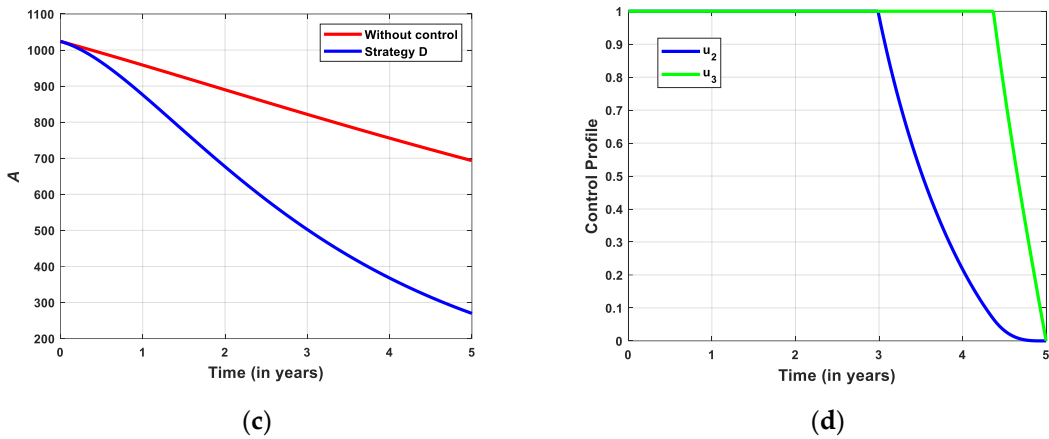

Figure 9. Simulation of the without control and with Strategy C on: (**a**) the number of I_u; (**b**) the number of I_a; (**c**) the number of A; (**d**) control profile of u_1 and u_3.

(**c**)   (**d**)

Figure 10. Simulation of the without control and with Strategy D on: (**a**) the number of I_u; (**b**) the number of I_a; (**c**) the number of A; (**d**) control profile of u_2 and u_3.

Table 3 presents the control strategies ranked in ascending order of total averted infections. Here, the ICER is calculated for Strategies B and D to enable a comparative evaluation of their relative effectiveness, defined as:

$$\text{CER}(B) = \frac{TC(B)}{TA(B)} = \frac{4.0169}{4.7007} = 0.8545.$$

$$\text{ICER}(D) = \frac{TC(D) - TC(B)}{TA(D) - TA(B)} = \frac{526.3404 - 4.0169}{25999.8318 - 4.7007} = 0.0201.$$

$$\text{ICER}(A) = \frac{TC(A) - TC(D)}{TA(A) - TA(D)} = \frac{526.4049 - 526.3404}{25999.9067 - 25999.8318} = 0,8612$$

$$\text{ICER}(C) = \frac{TC(C) - TC(A)}{TA(C) - TA(A)} = \frac{344.4764 - 526.4049}{26013.4355 - 25999.9067} = -13.4475.$$

Table 3. Total averted infection, total cost, and ICER of Strategies B, D, A, and C.

Strategy	TA	TC	ICER
Strategy B: u_1, u_2	4.7007	4.0169	0.8545
Strategy D: u_2, u_3	25999.8318	526.3404	0.0201
Strategy A: u_1, u_2, u_3	25999.9067	526.4049	0.8612
Strategy C: u_1, u_3	26013.4355	344.4764	-13.4475

Table 3 presents a summary of the ICER calculations of Strategies B, D, A, and C. From the table, the comparison between Strategy B and Strategy D shows that the ICER of Strategy B is higher than that of Strategy D, indicating that Strategy B is both more costly and less effective. Consequently, Strategy B should be excluded from the set of alternative control intervention strategies competing for the same limited resources. Furthermore, the ICER for Strategies D and A are recalculated using the same procedure, as presented in the fourth column of Table 4.

Table 4. Total averted infection, total cost, and ICER of Strategies D, A, and C.

Strategy	TA	TC	ICER
Strategy D: u_2, u_3	25999.8318	526.3404	0.0202
Strategy A: u_1, u_2, u_3	25999.9067	526.4049	0.8612
Strategy C: u_1, u_3	26013.4355	344.4764	-13.4475

From Table 4, the comparison between Strategy D and Strategy A shows that the ICER of Strategy A is higher than that of Strategy D, which indicates that Strategy A is both more costly and less effective. Consequently, Strategy A should be excluded from the set of alternative control

intervention strategies competing for the same limited resources. Furthermore, the ICER for Strategies D and C are recalculated, with the results presented in the fourth column of Table 5.

Table 5. Total averted infection, total cost, and ICER of Strategies D and C.

Strategy	TA	TC	ICER
Strategy D: u_2, u_3	25999.8318	526.3404	0.0202
Strategy C: u_1, u_3	26013.4355	344.4764	-5.3685×10^{-5}

The comparison of ICER values for intervention Strategies D and C, as shown in Table 5, indicates that the ICER for Strategy D is higher than that of Strategy C. Consequently, Strategy D is excluded from the set of remaining alternative strategies to prevent the inefficient allocation of limited resources. We observed that Strategy C, which involves the simultaneous implementation of educational campaigns and antiretroviral treatment measures (i.e., $u_1 \neq 0, u_3 \neq 0$ and $u_2 = 0$), is identified as the most cost-effective among the four proposed control strategies aimed at reducing and controlling the spread of HIV/AIDS in the community considered in this study.

5. Conclusions

In this study, we developed a mathematical model for HIV/AIDS dynamics using a system of seven nonlinear differential equations. The study incorporated educational campaigns for susceptible, screening of unaware infectives, and antiretroviral treatment formulated to describe the dynamics of HIV transmission with a saturated incidence. We performed a detailed mathematical analysis of our model, including the proof of positivity and boundedness of the model solutions, established using differential equation theory. By analyzing the system, we derive the effective reproduction number using the next-generation matrix method. The existence of the disease-free equilibrium point (DFE) and the endemic equilibrium point (EE) are shown. The EE components can be determined by substituting the positive real root of the cubic equations. When applied to cubic polynomials, Descartes' Rule of Signs allows one to determine the number of positive real roots. Based on the analysis, the Routh-Hurwitz criterion confirms the local stability of the DFE, while the application of center manifold theory reveals the presence of a forward bifurcation. Our bifurcation analysis demonstrates that the model consistently exhibits a forward bifurcation when the effective reproduction number is equal to one. The presence of a forward bifurcation also provides some information on the local stability of the endemic equilibrium. The global asymptotic stability of the DFE is established when the effective reproduction number is less than one, using the Castillo-Chavez method. Meanwhile, the global stability of the EE is analyzed through the Lyapunov function and LaSalle's Invariant Principle.

Based on the sensitivity analysis and numerical results, this study suggests that HIV infections can be reduced by lowering the contact rate and increasing the rates of screening, educational campaigns, and antiretroviral treatment. To mitigate HIV transmission, multiple time-dependent optimal control strategies are considered, including educational campaigns (ABC strategy), screening of unaware infected individuals, and antiretroviral treatment of aware infected individuals. A thorough analysis of the model is performed to explicitly establish the existence and characterize the optimal control triple using optimal control theory, guided by the Pontryagin Maximum Principle (PMP). To achieve a comprehensive understanding of the impact of three time-dependent functions on HIV/AIDS transmission dynamics, all possible control combinations are systematically categorized into four strategies. The results indicate that various combinations of control measures can significantly reduce the number of infective individuals in the population. Furthermore, the cost-effectiveness analysis using ICER identifies the combination of educational campaigns and antiretroviral treatment of aware infective individuals (Strategy C) as the most cost-effective intervention among the four strategies examined.

This study employs a classical-order optimal control model, but research shows that fractional-order models more effectively capture real-life phenomena. Future work will extend the model to a fractional-order framework to account for memory effects in HIV/AIDS transmission dynamics.

References

1. World Health Organization (WHO): Global strategic direction on HIV/AIDS 2024. Available online: https://www.who.int/observatories/global-observatory-on-health-research-and-development/analyses-and-syntheses/hiv-aids/global-strategic-direction (accessed on 17th February 2025).

2. UNAIDS. (2024). Global HIV & AIDS statistics-Fact sheet. Joint United Nations Programme on HIV/AIDS. https://www.unaids.org/en/resources/fact-sheet (accessed on 17th February 2025).

3. Bekker, L.G.; Beyrer, C.; Quinn, T. C. Behavioural and biomedical combination strategies for HIV prevention. *Cold Spring Harb. Perspect. Med*. **2012**, *2*, a007435. https://doi.org/10.1101/cshperspect.a007435

4. Joshi, H.R.; Lenhart, S.; Hota, S.; Agusto, F. Optimal Control of an SIR Model with Changing Behavior through an Education Campaign. *Electron. J. Differ. Equ*. **2015**, *50*,1-14. http://ejde.math.txstate.edu

5. Hota, S.; Agusto, F.; Joshi, H.R.; Lenhart, S. Optimal control and stability analysis of an epidemic model with education and treatment. *Conferensi Publication*, **2015**, 2015(special), 621-634. https://www.aimsciences.org/article/doi/10.3934/proc.2015.0621

6. Mukandavire, Z.; Garira, W. Effects of Public Health Educational Campaigns and the Role of Sex Workers on the Spread of HIV/AIDS among Heterosexuals. Theor. Popul. Biol. **2007**, *72*, 346-365. https://doi.org/10.1016/j.tpb.2007.07.002

7. Marsudi; Trisilowati; Suryanto, A.; Darti, I. Global stability and optimal control of an HIV/AIDS epidemic model with behavioral change and treatment. *Eng. Lett*. **2021**, *29*, 575-591. https://www.engineeringletters.com/issue_v29/issue_2/EL_29_2_26.pdf

8. Safiel, R.; Massawe, E.S.; Makinde, O.D. Modelling the effect screening and treatment on transmission of HIV/AIDS infection in a population. *Am. J. Math. Stat*. **2012**, *2*, 75-88. https://doi.org/10.5923/J.AJMS.20120204.03

9. Okosun, K.O.; Makinde, O.D.; Takaidza, I. Impact of optimal control on the treatment of HIV/AIDS and screening of unaware infectives. *Appl. Math, Modelling*, **2013**, 37, 3802-3820. https://doi.org/10.1016/j.apm.2012.08.004

10. Kateme, E.L.; Tchuenche, J.M.; Hove-Musekwa, S.D. HIV/AIDS Dynamics with Three Control Strategies: The Role of Incidence Function. *ISRN Appl. Math*. **2012**, 864795. https://doi.org/10.5402/2012/864795

11. Khan, M.A.; Ismail,M.; Ullah, S.; Farhan, M. Fractional order SIR model with generalized incidence rate. *AIMS Math*. **2020**, 5, 1856-1880. https://doi.org/10.3934/math.2020124

12. Khan, M.A.; Khan, Y.; Islam, S. Complex dynamics of an SEIR epidemic model with saturated incidence rate and treatment. *Physica A*. **2018**, 493, 210-227. https://www.sciencedirect.com/science/article/abs/pii/S0378437117310488

13. M. M. Ojo. Mathematical modelling of disease dynamics with saturated incidence and treatment response. *Math. Biosci*. **2021**, 340, 108686. http://doi.org/10.1016/j.mbs.2021.108686

14. Hu, Y.; Wang, H.; Jiang, S. Analysis and optimal control of a two-strain SEIR epidemic model with saturated treatment rate. *Mathematics* **2024**, 12, 3026. https://doi.org/10.3390/math12193026

15. Olaniyi, S.; Kareem, G.G.; Abimbade, S.F.; Chuma, F.M.; Sangoniyi, S.O. Mathematical modelling and analysis of autonomous HIV/AIDS dynamics with vertical transmission and nonlinear treatment. *Iran. J. Sci.* **2024**, *48*, 181-192. https://doi.org/10.1007/s40995-023-01565-w

16. Allali, K.; Balde, M.A.M.T.; Ndiaye, B.M. An optimal control study for a two-strain SEIR epidemic model with saturated incidence rates and treatment. *Discrete Dyn. Nat. Soc.* **2025**, *2025*, 8553106, 16 pages. https://doi.org/10.1155/ddns/8553106

17. Pontryagin, L.S.; Boltyanskii, V.G.; Gamkrelidge, R.V.; Mishchenko, E.F. *Mathematical Theory of Optimal Processes*, 1st edition, Routledge: London, 1987.

18. Lenhart, S.; Workman, J.T. Optimal Control Applied to Biological Models, 1st edition, Chapman and Hall/CRC: New York, 2007.

19. Yusuf, T.T.; Benyah, F. Optimal strategy for controlling the spread of HIV/AIDS disease: A case study of South Africa. *J. Biol. Dyn*. **2012**, 6, 475-494. https://doi.org/10.1080/17513758.2011.628700

20. Teklu, S.W. Investigating the effects of intervention strategies on pneumonia and HIV/AIDS co-infection model. *Biomed Res. Int.* **2023**, 5778209. https://doi.org/10.1155/2023/5778209

21. Teklu, S.W.; Terefe, B.B.; Mamo, D.K.; Abebaw, Y.F. Optimal control strategies on HIV/AIDS and pneumonia co-infection with mathematical modelling approach. *J. Biol. Dyn*. **2024**, *18*, 2288873. https://doi.org/10.1080/17513758.2023.2288873

22. Teklu, S.W.; Workie, A.H. A dynamical optimal control theory and cost-effectiveness analysis of the HBV and HIV/AIDS co-infection model. *Front. Public Health* **2024**, *12*, 1444911. https://doi.org/10.3389/fpubh.2024.1444911

23. Berhe, H.W.; Makinde, O.D.; Theuri, D.M. Co-dynamics of measles and dysentery diarrhea diseases with optimal control and cost-effectiveness analysis. *Appl. Math. Comput*. **2019**, *347*. https://doi.org/10.1016/j.amc.2018.11.049

24. Olaniyi, S.; Okosun, K.O.; Adesanya, S.O.; Lebelo, R.S. Modelling malaria dynamics with partial immunity and protected travellers: optimal control and cost-effectiveness analysis. *J. Biol. Dyn*. **2020**, *14*, 90-115. https://doi.org/10.1080/17513758. 2020.1722265

25. Asamoah, J.K.K.; Yankson, E.; Okyere, E.; Sun, G.Q.; Jin, Z.; Jan, R. et al. Optimal control and cost-effectiveness analysis for dengue fever model with asymptomatic and partial immune individuals. *Results Phys*. **2021**, *31*, 104919. https://doi.org/10.1016/j.rinp.2021.104919

26. Asamoah, J.K.K.; Okyere, E.; Abidemi, A.; Moore, S.E.; Sun, G.Q.; Jin, Z. et al. Optimal control and comprehensive cost-effectiveness analysis for COVID-19. *Results Phys*. **2022**, *33*, 105177. https://doi.org/10.1016/j.rinp.2022.105177

27. Appiah, R.F.; Jin, Z.; Yang, J.; Asamoah, J.K.K. Optimal control and cost-effectiveness analysis for a tuberculosis vaccination model with two latent classes. *Model. Earth Syst. Environ*. **2024**, *10*, 6761-6785. https://doi.org/10.1007/s40808-024-02128-7H.

28. Engida, A; Gathungu, D.K.; Ferede, M.M.; Belay, M.A.; Kawe, P.C.; Mataru, B. Optimal control and cost-effectiveness analysis for the human melioidosis model. *Heliyon* **2024**, *10*, e26487. https://doi.org/10.1016/j.heliyon.2024.e26487

29. Kang, T.L.; Huo, H.F. Dynamics and optimal control of tuberculosis with the combined effects of vaccination, treatment and contaminated environments. *Math. Biosci. Engin*. **2024**, *21*, 5308-5334. https://www.aimpress.com/journal/MBE

30. Smith, H.L.; Waltman, P. *The Theory of the Chemostat: Dynamics of Microbial Competition*, Cambride University Press: Cambride UK, 1995.

31. van den Driessche, P.; Watmough, J. Reproduction numbers and subthreshold endemic equilibria for compartmental models of disease transmission. Math. Biosci. **2002**, *180*, 29-48. https://doi.org/10.1016/S0025-5564(02)00108-6

32. Diekmann, O.; Heesterbeek, J.A.P.; Metz, J.A.J. On the definition and the computation of the basic reproduction ratio R0 in , 28odels for infectious diseases in heterogeneous populations. *J. Math. Biol*. **1990**, *28*, 365-382. http://doi.org/10.1007/BF00178324

33. Muthu, P.M.; Kumar, A.P. Optimal control and bifurcation analysis of SEIHR model for COVID-19 with vaccination strategies and mask efficiency. *Comput. Math. Biophys*., **2024**, *12*, 20230113. https://doi.org/10.1515/cmb-2023-0113

34. LaSalle, J.P. *The Stability of Dynamical System*, In: CBMS-NSF Regional Conference Series in Applied Mathematics, Pa: SIAM, Philadelphia, 1976.

35. Castillo-Chavez, C.; Song, B. Dynamical models of tuberculosis and their applications. *Math. Biosci. Eng.*, **2004**, *1*, 361-404. https://doi.org/10.3934/mbe.2004.1.361

36. Chitnis, N.; Hyman, J.M.; Cushing, J.M. Determining important parameters in the spread of malaria through the sensitivity analysis of a mathematical model. *Bull. Math. Biol*. **2008**, *70*, 1272-1296. https://doi.org/10.1007/s11538-008-9299-0

37. Fleming, W.H.; Rishel, R.W. *Deterministic and Stochastic Optimal Control*, Springer: New York, 1975.

38. Bector, C.R.; Chandra, S.; Dutta, J. *Principles of Optimization Theory*, Narosa Publishing House: New Delhi, 2005.

39. Abidemi, A.; Fatmawati, Peter, O. J. An optimal control model for dengue dynamics with asymptomatic, isolation, and vigilant compartments. *Decis. Anal. J.* **2024**, 10, 100413. https://doi.org/10.1016/j.dajour.2024.100413

40. Aldila, D.; Dhanendra, R.P.; Khoshnaw, S.H.A.; Puspita, J.W.; Kamalia, P.Z.; Shahzad, M. Understanding HIV/AIDS dynamics: insight from CD4+T cells, antiretroviral treatment, and country-specific analysis. *Front. Public Health* **2024**, *12*, 1324858. https://doi.org/10.3389/fpubh.2024.1324858